

## Hybrid Dy-NFIS & RLS equalization for ZCC code in optical-CDMA over multi-mode optical fiber

Alaan Ghazi <sup>1,2,3</sup>, S. A. Aljunid <sup>2</sup>, Syed Zulkarnain Syed Idrus <sup>1</sup>, Alaa Fareed <sup>4</sup>, Aras Al-dawoodi <sup>5</sup>, C. B. M Rashidi <sup>2</sup>, R. Endut <sup>2</sup>, N. Ali <sup>2</sup>, Aram Hewa Mohsin <sup>6</sup>, Sirwan Saber Abdullah <sup>7</sup>

<sup>1</sup> School of Human Development & Techno Communication, University Malaysia Perlis, Malaysia

<sup>2</sup> Faculty of Electronic Engineering Technology, University Malaysia Perlis, Malaysia

<sup>3</sup> Computer Technical Engineering, Al-Qalam university College, Iraq

<sup>4</sup> School of Computing, University Utara Malaysia, Malaysia

<sup>5</sup> Computer Science Department, College of Computer Science and Information Technology, Kirkuk University, Iraq

<sup>6</sup> Criminal Evidence Department Al-Qalam University College, Iraq

<sup>7</sup> Information Technology and Communication Department, Rafidain Bank, Iraq

### ABSTRACT

For long haul coherent optical fiber communication systems, it is significant to precisely monitor the quality of transmission links and optical signals. The channel capacity beyond Shannon limit of Single-mode optical fiber (SMOF) is achieved with the help of Multi-mode optical fiber (MMOF), where the signal is multiplexed in different spatial modes. To increase single-mode transmission capacity and to avoid a foreseen “capacity crunch”, researchers have been motivated to employ MMOF as an alternative. Furthermore, different multiplexing techniques could be applied in MMOF to improve the communication system. One of these techniques is the Optical Code Division Multiple Access (Optical-CDMA), which simplifies and decentralizes network controls to improve spectral efficiency and information security increasing flexibility in bandwidth granularity. This technique also allows synchronous and simultaneous transmission medium to be shared by many users. However, during the propagation of the data over the MMOF based on Optical-CDMA, an inevitable encountered issue is pulse dispersion, nonlinearity and MAI due to mode coupling. Moreover, pulse dispersion, nonlinearity and MAI are significant aspects for the evaluation of the performance of high-speed MMOF communication systems based on Optical-CDMA. This work suggests a hybrid algorithm based on nonlinear algorithm (Dynamic evolving neural fuzzy inference (Dy-NFIS)) and linear algorithm (Recursive least squares (RLS)) equalization for ZCC code in Optical-CDMA over MMOF. Root mean squared error (RMSE), mean squared error (MSE) and Structural Similarity index (SSIM) are used to measure performance results.

**Keywords:** MMOF, Optical-CDMA, Dy-NFIS, RLS, SMOF, Equalization, Pulse dispersion, Nonlinearity and MAI.

### Corresponding Author:

Alaan Ghazi  
School of Human Development & Techno Communication  
University Malaysia Perlis  
Perlis, Malaysia  
[alaanghazi@gmail.com](mailto:alaanghazi@gmail.com)

### 1. Introduction

The Internet based telecommunication infrastructure uses optical fiber for backbones [1], with the tremendous growth in the Internet traffic. Its bandwidth increasing demand for numerous applications is the hard reality of today [2, 3]. Therefore, enhancing the capacity for fiber optic is a necessary requirement to transfer larger amount of data. The techniques used to raise the data transmission capacity for fiber optic communication are

Time Division Multiple Access (TDMA), Orthogonal Frequency-Division Multiple Access (OFDMA) and Wavelength Division Multiple Access (WDMA). However, a large data remained to be transmitted by these techniques to fulfill the future needs of the end users, due to the high capacity of data projected and the existing optical transmission channel that operates over Single Mode Fiber (SMF) reaching their fundamental capacity limits [4, 5]. However, a channel capacity beyond the Shannon limit of SMF can be achieved with the help of Multi-Mode Optical Fiber (MMOF), where the signal is multiplexed in different spatial modes [5, 6]. Optical-CDMA simplifies and decentralizes network control to improve spectral efficiency and information security, which increase flexibility in bandwidth granularity and allows synchronous and simultaneous transmission medium to be shared by many users. This topic has received more attention in recent years. However, during propagation of data over the MMOF based on Optical-CDMA, an inevitable issue encountered is pulse dispersion, nonlinearity and MAI due to mode coupling [7-11]. The most important impairment of Optical-CDMA is dispersion of pulse which causes MAI [9]. This dispersion is a time-varying phenomenon caused by the variation in the propagation constants of a fiber which is called mode dispersion with a time-varying phenomenon [8, 11-15]. It is the most critical impairment of Optical-CDMA and must be compensated to avoid data MAI [9]. Optical-CDMA system is common because of the excess in bandwidth allowing users to send data on optic cable using various techniques in the fiber optic. At high data rates, the pulse dispersion and MAI [16] are created by the effect of optical signal dispersion [14]. In case of optical communication, the focus is on negating the dispersion, which is chromatic, polarization and electrical [11, 13, 17-19]. To improve pulse dispersion, different approaches are used to recover signal [20, 21] in optical communication system such as space diversity, equalization and coding for reducing the effects of fading and MAI [22]. One of those methods is known as equalization used to eliminate or reduce the effects of MAI [23]. Minimum Mean Square Error (MMSE) filters [21, 24], Fast Fourier Transform (FFT) [25, 26], Finite Impulse Response (FIR) [3], Constant Modulus Algorithm (CMA) and (RLS) [13] are tapped filters some equalization for Optical-CDMA. They are intended for linear equalization. However, the existing equalization schemes suffer from undesirable excess MSE during training due to channel non-linearity, distortion and additive noise that affect the performance of linear equalizer. At the receiver, there is no sufficient linear equalizer for performances because there is a chromatic dispersion and VCSEL nonlinearities [27]. In the previous studies, equalization is the method utilized to compensate and reduce the transmission introduced distortion in fiber communications systems. This could be any process of operation of the signal minimization of distortion and ISI. Equalization aims to provide communications without errors through ensuring that transmitted signals over the link recovered by the side of the receiver as an original signal. Moreover, there are different equalizations implemented for Optical-CDMA. As Table 1 below reviews, there is an equal Optical-CDMA. Optical fiber strives as a robust technique in communication system because optical communication can handle huge data with high speed for a long haul and local area network. Optical-CDMA transmissions are attractive because it can transmit different users in a secure way that can be used in a single optical. However, in the data propagation over the optical communication based on Optical-CDMA, an inevitable issue encountered is ISI and MAI which stems from the mode coupling [21, 25]. Equalization can be used to eliminate or reduce the effects of ISI [23, 28]. According to Table 1, which shows different equalization schemes that have developed for Optical-CDMA, it is mostly dependent on tapped filters intended for linear equalization. The tuneable dispersion of the signal data ultra-short carrier pulses spread by the fibre optic cable is a valid method for solving this problem, [19]. The use of inbound pulses by the chirp control based on clock power can improve the transmission system performance. However, the drawbacks of this technique based on SMF and for short range are first order mode dispersion that is possible in overcoming the nonlinear dispersion. Two signal processing methods for decreasing ISI are proposed. The first method is the use of an adaptive M-ary pulse-amplitude modulation (M-PAM) scheme[21]. This scheme has a high bandwidth efficiency allowing a high data through sending low-rate information. The second is diminishing ISI and MAI simultaneously while optimizing the SINR by transmitting waveforms and MMSE filters is designed known as joint optimal pulse shaping. The results show that both of

the schemes can support multiuser VLC systems with high-speed data transmission. However, this system uses optimization based on linear filter, which is used, for short range in Optical-CDMA over VLC.

Table 1. Existing equalization techniques in OPTICAL-CDMA

No	Op-Link	Challenges	Cite
1	17 Km SMF	Chromatic dispersion	[19]
2	VLC	MAI, ISI	[21]
3	VLP	MAI	[25]
4	150 KM SMF	pulse dispersion	[13]
5	VLC	MAI	[24]
6	VLC	MAI	[29]
7	20 KM SMF	MAI	[29]
8	OPTICAL-CDMA –PON fiber	MAI	[16]
9	24 users SMF	MAI	[18]
10	indoor	ISI	[30]

Moreover, the use of a central unit helps to avoid signal interferences from various transmitters in the system of visible light positioning (VLP). In this paper, the author [25] suggests an uncoordinated multiple access scheme for systems the VLP without requiring a central unit. Each transmitter is equipped with a light-emitting diode (LED) assigned a unique code. The code words are sent at different times by each trainmaster. By the use of Fast Fourier Transform (FFT), a receiver can reduce the interference among the LEDs to estimate the average power received from each LED, which is also used for position estimation. However, the enhancement of the system based on the filter FFT to avoid the interference among the signal for a short-range channel. The first-order modal dispersion can be compensated successfully by linear signal processing. Higher-order modal dispersion that occurs over long distances and high capacity can contribute to the nonlinear signal distortion and ISI that cannot be compensated successfully by linear signal processing [31-33]. The literature on telecommunication providers is forced to increase the performance of fiber networks through the improvement of the channel multiplexing techniques and the increase of spectral efficiency in a channel because of the growing bandwidth demands [13]. The most serious fiber network impairment is pulse dispersion, which could happen because of the chromatic dispersion. This dispersion is different wavelength travel speeds because of the polarization and mode dispersion (PMD)-the difference in the fiber propagation constants compensated to avoid ISI. For the reduction of the impact of CD PMD, the study applies Constant Modulus Algorithm (CMA) and RLS. However, a linear equalization used in this study based on linear dispersion occurs in simple signal mode fiber (SMF) which is first-order modal dispersion. Furthermore, according to, [24] a partially joint optimized power allocation is compared with a weighted distributed power. These two compared elements are two algorithms with the various distribution. CDMA plus optical on-off keying (OOK) and MMSE receiver are used for reducing the MAI effect in the domestic VLC system. However, the MMSE filter has been used as equalizer for indoor VIC network, which has less noise, which is called linear dispersion than can be compensated by MMSE filter. However, outdoor long communication incurs nonlinear dispersion. Based on [29], the author investigates offline DSP at the receiver side by down-converting the received signal to baseband. When CP is removed and serial to parallel (S/P), Fast Fourier Transmission (FFT) is utilized for transforming the baseband time-domain MC-CDMA signal to the domain of frequency. In addition, to estimate the channel and recover the data, post-equalization algorithms are utilized. Because of the system, an OFDM-based transceiver is used. Each receiver FFT output is a narrow-band signal. This signal is equalized through the multiplication of a simple complex constant. However, the pre-and post-equalization have been implemented based on simple noise that can be recovered using simple filter. The authors [16] have used different detections based on PPIC, DEC, EM, and the MMSE detectors for the improvement of the limitation in Optical-CDMA which is MAI. However, different detections based on complexity are compared. Therefore, the system performance is reduced quickly as the users and bandwidth increase for long-distance. This increase raises complexity. One of the major limitations of an optical fiber is its effects on data-carrying capacity and the

reduction of the overall performance in addition to dispersion. To compensate for the chromatic dispersion in a multiuser Optical-CDMA, Electronic Equalization Technique (EET) is proposed. However, the filter that has been proposed based on a simple filter is the liner. The selection of pre-and post-equalization-based subcarrier to transmit power reduction in the downlink transmissions is analyzed to solve the average transmit optical power reduction issue in the MC-CDMA domestic optical wireless communications by the use of intensity modulation. Also, the direct detection shows that pre-equalization performance is usually better than post-equalization concerning BER for the same optical transmit power [30]. Higher-order modal dispersion can contribute to the nonlinear signal distortion and ISI cannot be compensated successfully by linear signal processing [31, 32, 34]. Additionally, the transmission grows over longer distances; the nonlinear intersymbol interference caused by the dispersion phenomena influences the data. Nonlinear distortion in optical communication systems and other communication systems can be solved with the help of equalization [23, 28]. According to Table 1, the different equalization schemes that have been developed for Optical-CDMA are mostly based on tapped filters such as RLS, CMA, MMSE, and FFT classified under linear equalization. The previous equalization can tackle the linear problem, but unfortunately, it cannot compensate for the nonlinear problem [31]. The nonlinear influence of the optical fiber happens for two reasons: (1) the medium refractive index intensity dependence and (2) the inelastic-scattering phenomenon as in any other physical systems [35]. As presented in [34] in the first order, the input-output intensity waveforms relationship is linear. However, the higher-order influence makes the relationship nonlinear as in SMF with higher-order PMD and chromatic dispersion (CD). The higher-order modal dispersion can contribute to the nonlinear signal distortion and ISI that cannot be compensated successfully by linear signal processing [31] and the adaptive algorithms will tend to experience undesirable local minima in the training mode [36, 37]. These drawbacks of the linear models have motivated the study to adopt the hybrid nonlinear and linear models based on hybrid equalization in MMF to mitigate ISI and to make improvement to the channel impulse response. Responding to the discussions in the previous paragraphs, this study will emphasize on linear and non-linear adaptive equalization. The information size of optical communication networks has widely improved in the past four decades because of introducing and developing coherent detection, advanced modulation formats, optical amplifiers, and digital signal processing techniques. These developments cause a revolution in the optical communication systems. In addition, the Internet increases long-distance transmissions and high-capacities. Transmission impairments could be Kerr fiber nonlinearity laser phase noise, chromatic dispersion, and polarization mode dispersion degrading the long-haul high-capacity optical fiber communication system. Machine learning is a recent development in optical communications that could become a key enabler to develop future intelligent networks. For example, the techniques of powerful machine learning could cognitively operate at the physical levels and adaptive, low complexity transceiver units with advanced signal equalization. It could also function on monitoring, and digital encoding capabilities to higher layer node architectures and network topologies. This function can estimate future conditions of the network, demands of traffic, failures of connectivity, and threats of security, and accordingly to self-optimize their operation. Responding to the discussions in the previous paragraphs, this study emphasizes linear and non-linear adaptive equalization. It suggests a new way for Optical-CDMA by using hybrid equalization. The nonlinear algorithm based on the Dy-NFIS algorithm offline learning process first clusters the data to find cluster centers, each of which has a created fuzzy rule as antecedent depends on the cluster center. In addition, the consequence is based on a linear function trained by the vector of that input. The output is derived from activated rules for each training input through back-propagation by adjusting the MF and the consequence of the activated rules minimizes errors [38]. In short, under Dy-NFIS, Gaussian MF replaces the triangular MF and optimizes the model further using back-propagation [38]. Moreover, DENFIS online learning and Dy-NFIS offline learning processes have been applied in different applications such as mobile robot navigation and object tracking [39], dynamic time series prediction [40], Risk Analysis of Pest Insect Establishment [41], prediction error of MacKay glass dataset [38], rainfall-runoff (R-R) modeling [42] online detection “Zero-day” phishing email [43]. Modeling hourly dissolved oxygen concentration[44], fault density prediction in aspect-oriented systems[45], ICMPv6 flood attack detection[46], Spam E-mail Filtering [47], Rainfall-runoff modeling [48] and Mortality Prediction [49]. The other algorithm depends on the

linear such as RLS, CMA, and LMS, which are used for reducing the impact of PMD and CD. The RLS can be supervised and blinded which recursively obtains the filter coefficients minimizing a weighted linear least-squares cost function linked and input signals. The RLS filter converges to the same optimal filter coefficients similar to the Wiener filter of stationary signals [50]. It also tracks the time changes for non-stationary signals. This method is beneficial for many applications such as speech channel equalization, enhancement, radar with the filter and echo cancellation. It can also track relatively quick signal processing shifts [51] and can be useful in slowly changing environment. In the RLS algorithm, some primary input signal filter states and successive samples are utilized for the adaption of the filter coefficients [52]. In this paper, we developed a hybrid algorithm based on nonlinear algorithm ((Dy-NFIS) and linear algorithm ((RLS) equalization for ZCC code in Optical-CDMA over Multi-Mode Optical Fiber.

## 2. System description and proposed hybrid algorithm

In this paper, the representation of the hybrid Dy-NFIS and RLS equalization for ZCC code in Optical-CDMA over Multi-Mode Optical Fiber (MMOF) shown in Figure 1 will be explained in four stages.

### 2.1. Optical code division multiple access (Optical-CDMA) over MMOF

The two first stages illustrating a block diagram of the Optical-CDMA system for three users 1D Zero Cross-Correlation (ZCC) codes for Optical-CDMA are based on three Laguerre-Gaussian modes over multi-mode optical fiber (MMOF) transmission system as explained in Figure 1 (a), and (b). They have been designed and simulated by the use of optical-system [53, 54] and MATLAB [55, 56] software. It is composed of three parts – transmitter, MMOF, and receiver. The parts of transmitter consist of Spatial VCSEL, Encoding, PRBSG, NRZ pulse generator, and Power Combiner) components. Moreover, spatial VCSEL power is set to 1 dBm with different code weights. At 1.866 Gbps, a different set of modes is generated with different Laguerre-Gaussian modes are LG 0 1, LG 0 2, and LG 0 3 modes as shown in Figure 2 where LG modes are described mathematically as [57]. Here we define  $\psi_{m,n}(r, \varphi)$  as follows:

$$\psi(r, \varphi) = \left( \frac{2r^2}{W_0^2} \right)^{\frac{|n|}{2}} L_m^n \left( \frac{2r^2}{W_0^2} \right) \exp \left( -\frac{r^2}{W_0^2} \right) \exp \left( j \frac{\pi r^2}{\lambda R_0^2} \right) \begin{cases} \sin(|n|\varphi), n \geq 0 \\ \cos(|n|\varphi), n < 0 \end{cases} \quad (1)$$

Here,  $W_0$  is spot size,  $R$  refers to the radius of curvature, and  $L(n, m)$  is the Laguerre Polynomial. Also,  $n$  and  $m$  represent Y (the radial index) and X (the azimuthal index) indexes, respectively. Furthermore, ZCC code can usually be used in Optical-CDMA because it has a zero-correlation feature. A high code cardinality is taken into consideration to design an optimal ZCC set (with excellent auto and cross-correlation features) and to maximize possible user numbers (and minimum code weight and code length). Accordingly, minimizing error probabilities and a guaranteed QoS can be achieved [58]. Recently, on systems based on Optical-CDMA, ZCC is implemented for Spectral Amplitude Coding (SAC) [59-62]. In this paper, the codes are generated at the encoder by assigning the wavelengths. The wavelengths are chosen according to a unique code given to every user, as shown in Figure 2 three users based on ZCC code. According to the given data and N.R.Z., Mach Zehnder Modulator (MZM) is utilized for the modulation of the users' wavelengths. Then, each user's output will be combined and transmitted onto the MMOF. The second part is the optic fiber link, which is multi-mode Optical fiber (MMOF). MMOF which is the attenuation is assigned as 0.25 dB km. The core radius is set to 50 nm with a 9 km maximum distance link. The final part is the receivers. The input signal from MMOF is the Splitter of Power into three decoders and three users. In addition, the Photo-detector (PIN) converts the optical domain into the electrical domain. Therefore, Gaussian pulse shaping will be applied to implement the ideal signal in the communication system domain [63-68]. To implement the Gaussian pulse shaping, the number of channels and the number of exciting modes that will be collected from the Optical-CDMA system over multi-mode optical fiber must be determined. Moreover, putting the channels into different time slots prevents the interference that may occur between channels and may cause ISI and optical nonlinear phenomenon. The

Gaussian function can be represented:

$$f(x) = \frac{1}{\sigma\sqrt{2\pi}} e^{-(x-\mu)^2/(2\sigma^2)} \dots \dots \dots (2)$$

Here,  $x$  is the channel range of Gaussian and depends on the number of modes at receiver,  $\mu$ , refers to mean or distribution expectation and its median of channel and  $\sigma$  is the standard deviation. In the suggested Gaussian pulse shaping, the Sigma parameter is  $\sigma = 2$ , the value of Sigma is the collected modes number and channels, whereas the Mean value is  $\mu = 9.5$  for each channel. These parameters are used in MATLAB for the production of three Gaussian pulse channels, which are mapped with the three channels collected from the MMOF. Moreover, from Figure 1 (a), and Figure 1 (b), it appears that the channel impulse response at the input state before multimode optical fiber system represents a different optical Gaussian pulse (ideal signal) for three users and three spatial visualizers of LG modes which are (LG 0 1, LG 0 2 and LG 0 3) as shown in Figure 2. The channel impulse response at the output state after multimode optical fiber system represent different distorted signal at distance 9 Km as shown in Figure 3. The result is three curves; these curves represent the Gaussian pulse shaping for the three channels and one curve for each. In addition, every channel has a specific time interval as a result no overlap will occur between these channels G1, G2, and G3 as in Figure 4. Hence, the collected distorted signal and Gaussian pulse shaping in its status are not suitable to apply the optimization process because they are in different ranges. To tackle this problem, data normalization processes are implemented based on the Min-Max normalization method to make this data suitable for optimization in this research. Moreover, data is normalized in both the distorted signal and Gaussian pulse shaping. In this normalization, the distorted signal should be fitted with the Gaussian pulse shaping or be in the same range. This work utilizes a linear normalization. The data min and max values are 0 and 1. The normalization process is applied to both distorted signal i.e (the distorted signal from the Optical-CDMA model) and the Gaussian signal.

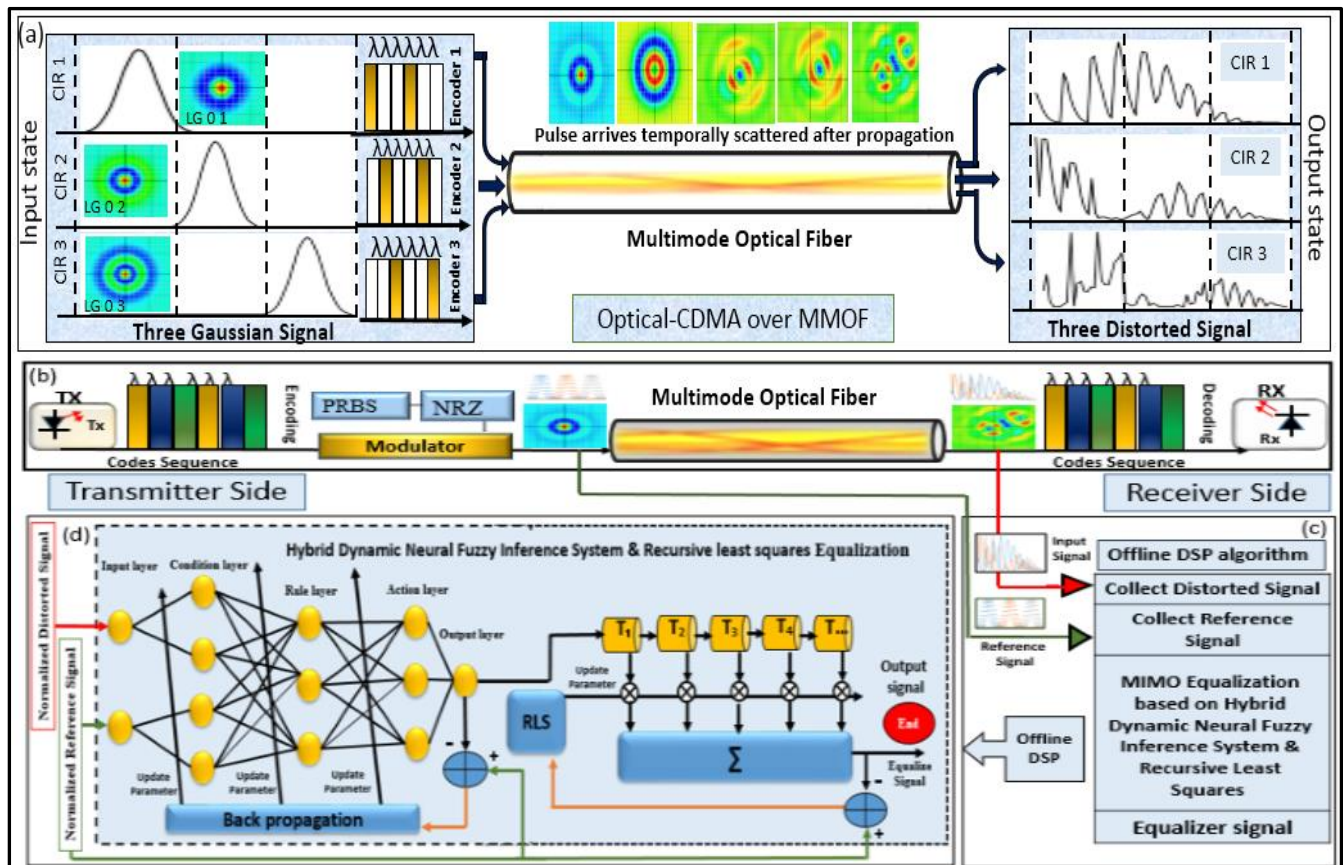


Figure 1. Optical-CDMA over multimode optical fiber modal



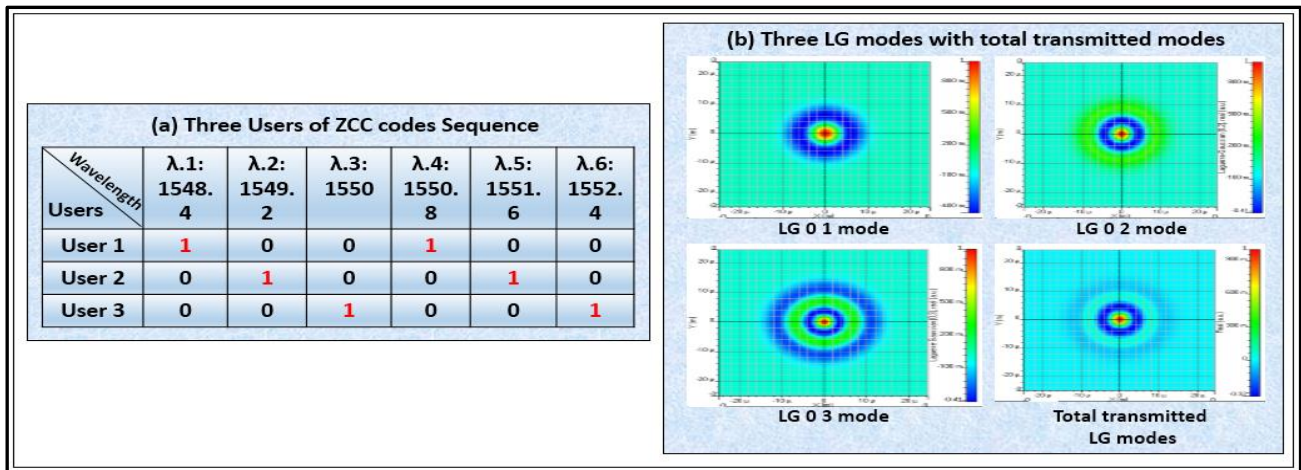


Figure 2. Illustrating three users with three modes in Optical-CDMA over MMOF

The channel impulse response at the input state before the multimode optical fiber system represents different optical Gaussian signals (ideal signals) for three users and three spatial visualizers of LG modes. The channel impulse response at the output state following a multimode optical fiber system represents a different distorted pulse (b). Optical-CDMA over MMOF is based on LG modes with different optical Gaussian Pulse shaping based on ZCC codes, (c). The steps of the hybrid equalization are shown (d). The hybrid nonlinear and linear equalization are presented:

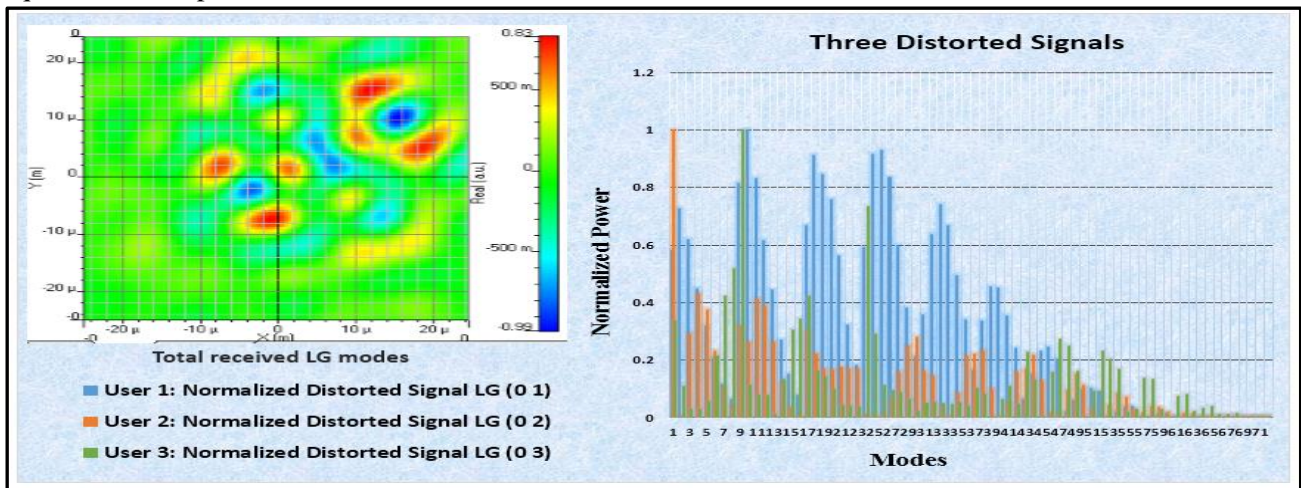


Figure 3. Power coupling and pulse broadening of three users in Optical-CDMA after MMOF at distance 9 Km

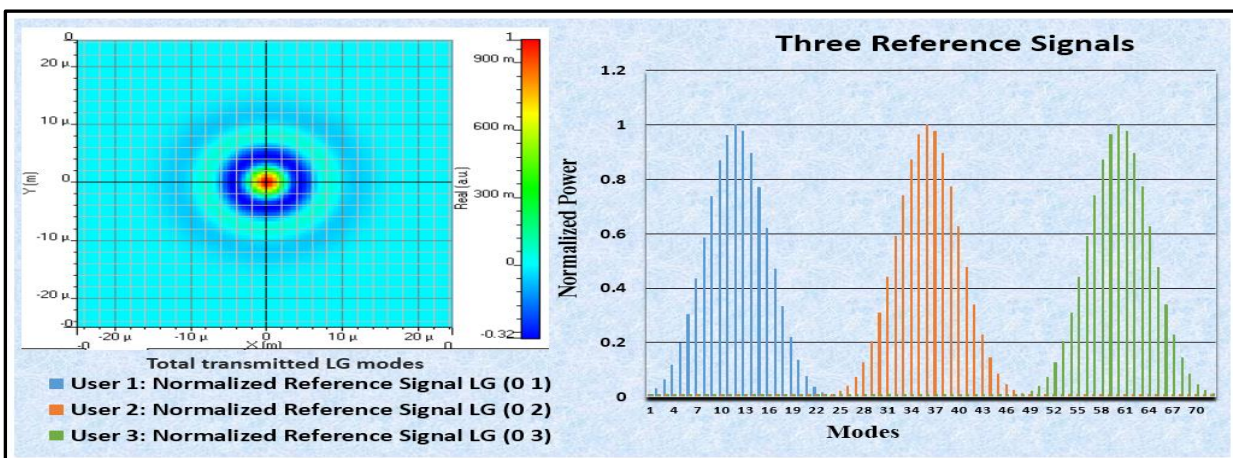


Figure 4. Normalized reference signal at the input state before multimode optical fiber system represents different optical Gaussian pulse (ideal signal) for three users and three spatial visualizers of LG modes which are (LG 0 1, LG 0 2, and LG 0 3) modes

## 2.2. Proposed hybrid nonlinear and linear algorithm

To apply a hybrid algorithm for the Optical-CDMA system, we need the three distorted signals and three reference signals to be inserted into the hybrid equalization. In this paper, we use the nonlinear and linear algorithms are explained in more detail in the nest sub-Sections.

### 2.2.1. Nonlinear algorithm

An online local model which is Dynamic Evolving Neural Fuzzy Inference System (DENFIS) is proposed [40]. Takagi-Sugeno (TS) fuzzy inference system (FIS) is made by the algorithm [69, 70]. In this system, the fuzzy rules are made according to the input vector clustering results. The system progresses by the cluster and rule updates when the new input vectors enter the system. This is one of the reasons for the performance of DENFIS and an online algorithm because this technique includes various sub-groups of the data points representing the same features developing a rule for each of the subgroups. Online algorithms [71, 72] analyze each piece of input data separately. In addition, they usually attempt to quickly process the usage and speed of minimal memory because they made to process data streams. For this purpose, the algorithm complexity often reduces the input data that are discarded once analyzed. On the other hand, the offline algorithm [73-75] is capable of processing the whole dataset. This often better predicts accuracy because there are more data for the algorithm. Because DENFIS was o invented as an online algorithm. The FIS and learning techniques fulfill the expectations while DENFIS offline is designed with an online version of DENFIS. This design reduces the dynamic evolving DENFIS algorithm feature and is substituted by a more sophisticated learning algorithm. This accuracy of the logarithm is proved; however, there could be more applications of optimization to increase accuracy. In the original DENFIS algorithm, the antecedents are produced according to the cluster centers and the outcomes are made based on the samples close to the cluster centers. For the reduction of the computational complexity, a triangular membership function was utilized. This work designs an improved offline DENFIS version extending the original algorithm with better in-depth learning. The Dy-NFIS “is a nonlinear offline learning process algorithm”. The algorithm, Dy-NFIS, and Gaussian MF substitute the triangular MF. Since it grows with no limits, Gaussian MF produces a better cover of the problem space and the gaps which could be introduced by triangular MF because there could be an elimination of its finite range. In addition, Dy-NFIS optimizes the antecedents and outcomes by the use of back-propagation the error reduction in the active rules. In these improvements, Dy-NFIS could be be more accurate because of the back-propagation caused by its Gaussian MF. Thus, it is more appropriate for real applications that are not critical in terms of time.

The DyNFIS offline learning process could be as follows:

- 1- Clustering the data using Fuzzy c-means (FCM)
- 2- For each cluster, m fuzzy rule is created.
- 3- Based on each cluster’s center position, an antecedent is created.
- 4- The consequence is measured through a linear function with cluster samples.
- 5- For each testing sample, the output is derived from the rules followed by adjusting the fuzzy membership function and the consequence by backpropagation for reducing the errors.
- 6- The third step is repeated for multiple epochs/till the required accuracy is achieved.

For example, data consist of N data pairs, variables of P input and one variable of output  $\{[x_{i1}, x_{i2}, \dots, x_{ij}], y_i\}$ ,  $i = \{1, 2, \dots, N\}$ ,  $j = \{1, 2, \dots, P\}$ . The m fuzzy rules can be explained by procedure of cluster. The lth rule is as follows:

R<sub>l</sub>: If x<sub>1</sub> is about F<sub>l1</sub> and x<sub>2</sub> is about F<sub>l2</sub> ... x<sub>p</sub> is about F<sub>lp</sub> and then

$$n_i = \beta + x_1\beta_1 + x_2\beta_2 + >>> + x_p\beta_p \dots\dots\dots (3)$$

F<sub>lj</sub> are the fuzzy sets explained by the Gaussian membership function (MF):

$$\text{Gaussian MF} = \alpha \exp \left[ -\frac{(x-m)^2}{2\sigma^2} \right] \dots\dots\dots (4)$$

By the modified procedure of the center average defuzzification, the output value is measured for an input vector  $x_i = [x_1, x_2 \dots x_p]$ :



$$f(x_i) = \frac{\sum_{i=1}^M n_i \prod_{j=1}^p \alpha_{ij} \exp(-\frac{(x_{ij} - m_{ij})^2}{2\sigma_{ij}^2})}{\sum_{i=1}^M \prod_{j=1}^p \alpha_{ij} \exp(-\frac{(x_{ij} - m_{ij})^2}{2\sigma_{ij}^2})} \dots \dots \dots (5)$$

DyNFIS is given a training pair of input and output  $[x_i, t_i]$ . The system reduces the next objective function:

$$E = \frac{1}{2} [f(x_i) - t_i]^2 \dots \dots \dots (6)$$

The backpropagation which is the steepest descent algorithm is utilized for obtaining the formulas (7)-(13) to

$$\text{optimize the parameters } n_i, \alpha_{ij}, m_{ij}, \sigma_{ij}, \text{ and } \beta_i m_{ij}(k+1) = m_{ij}(k) - \frac{\eta_{ij} \Phi(x_i) [f^{(k)}(x_i) - t_i]}{\sigma_{ij}^2(k)} \dots \dots \dots (7)$$

$$x[n_i(k) - f^{(k)}(x_i)][x_{ij} - m_{ij}(k)]$$

$$n_i(k+1) = m_{ij}(k) - \eta_{ij} \Phi(x_i) [f^{(k)}(x_i) - t_i] \dots \dots \dots (8)$$

$$\alpha_{ij}(k+1) = \alpha_{ij}(k) - \frac{\eta_{\alpha} \Phi(x_i) [f^{(k)}(x_i) - t_i]}{\alpha_{ij}(k)}$$

$$x[n_i(k) - f^{(k)}(x_i)] \dots \dots \dots (9)$$

$$\sigma_{ij}(k+1) = \sigma_{ij}(k) - \frac{\eta_{\sigma} \Phi(x_i) [f^{(k)}(x_i) - t_i]}{\sigma_{ij}(k)}$$

$$x[n_i(k) - f^{(k)}(x_i)][x_{ij} - m_{ij}(k)]^2 \dots \dots \dots (10)$$

$$\Phi(x_i) = \frac{\prod_{j=1}^p \alpha \exp(-\frac{(x_{ij} - m_{ij})^2}{2\sigma_{ij}^2})}{\sum_{i=1}^m \prod_{j=1}^p \alpha \exp(-\frac{(x_{ij} - m_{ij})^2}{2\sigma_{ij}^2})} \dots \dots \dots (11)$$

$$\beta_{10}(k+1) = \beta_1(k) \eta_{\beta} \Phi(x_i) [f^{(k)}(x_i) - t_i] \dots \dots \dots (12)$$

$$\beta_{ij}(k+1) = \beta_1(k) \eta_{\beta} \Phi(x_i) [f^{(k)}(x_i) - t_i] x_{ij} \dots \dots \dots (13)$$

Where  $\eta_m, \eta_n, \eta_{\alpha}, \eta_{\sigma}$  and  $\eta_{\beta}$  are learning rates for updating the parameters:  $n_i, \alpha_{ij}, m_{ij}, \sigma_{ij}$ , and  $\beta_i$  respectively  
In Dy-NFIS algorithm, the below indexes are employed:

Training data points are  $i=1, 2, \dots, N$ ; input variables:  $j=1, 2, \dots, P$ ; fuzzy rules:  $l=1, 2, \dots, M$ ; training iterations:  $k=1, 2, \dots$

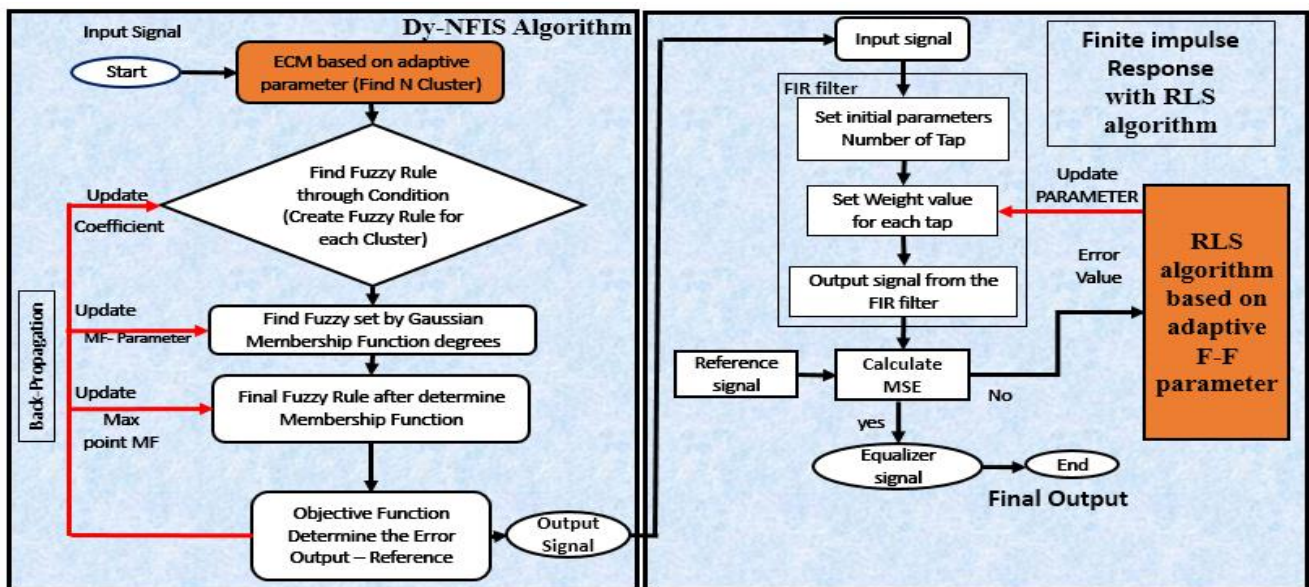


Figure 5. The flowchart of the hybrid algorithm (nonlinear algorithm (Dy-NFIS)) and linear algorithm (RLS) equalization.

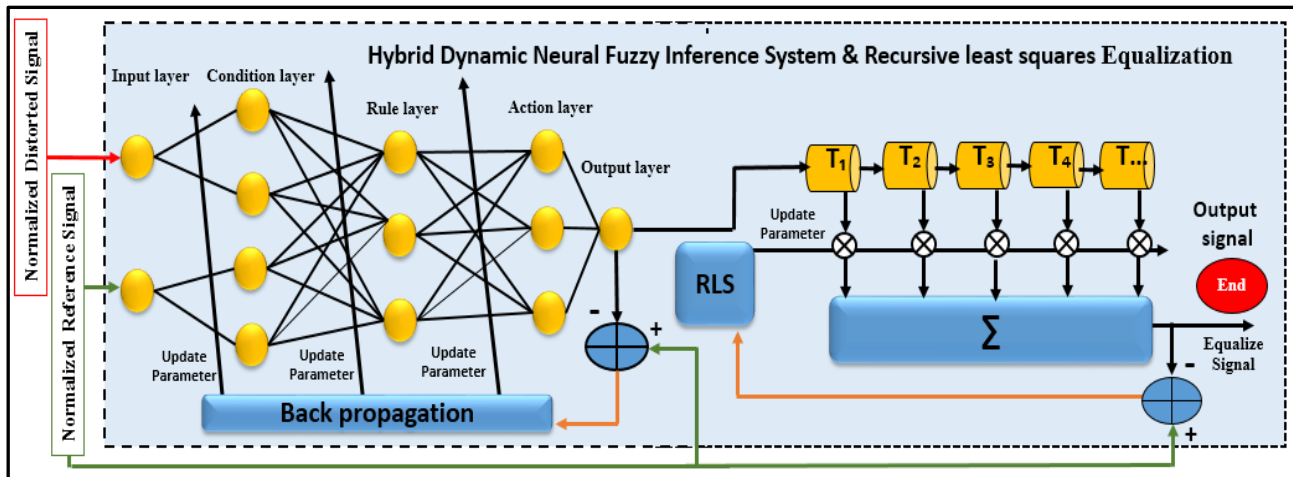


Figure 6. The block diagram of the hybrid algorithm (nonlinear algorithm (Dynamic evolving neural fuzzy inference) and linear algorithm (Recursive least squares) equalization

The development and implementation of the Dy-NFIS equalization approach will be processed by using MATLAB, the nonlinear algorithm based on Dy-NFIS, and evolving clustering method (ECM) algorithm will be applied to the (off-line learning). Dy-NFIS was proposed by [38], as it combines both neural network and fuzzy logic to introduce a powerful hybrid method by taking an advantage of the adaptive learning capability of neural networks and the reasoning capability of fuzzy logic. Dy-NFIS is known by the MFs and rules incrementally from data using evolving clustering method (ECM) algorithm. The ECM (Song and Kasabov 2001b) is a distance-based grid partitioning method due to its incremental nature through a one-pass process which by including constrained minimization criteria can also be used offline. The fuzzy inference system (FIS) that will be utilized is a first-order Takagi-Sugeno-Kang (TSK). Moreover, at the beginning of the learning process [76]. The flowchart of the ECM algorithm and the following explains this [77] as shown in Figure 7.

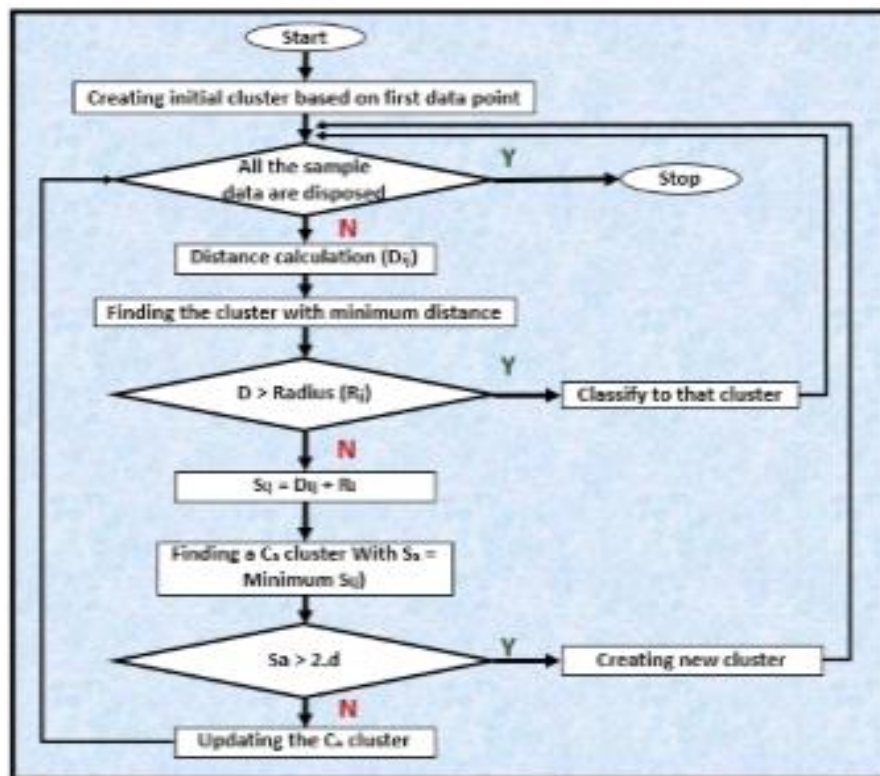


Figure7. Flowchart of ECM

- The number of M clusters is generated by executing the ECM on the input vector of the initial data (n). Then, for each cluster, the closest points are determined. The distance determination is generally defined concerning

general Euclidean distance. Therefore, assuming the consideration of the center of a cluster ( $c$ ) and position of example point ( $x$ ), the distance between them ( $D_{ij}$ ).

- The general trend of determining the point for each cluster is in accordance with the concept of the maximum distance between each point and the cluster center, and its comparison with a threshold value ( $d$ ).
- If the calculated distance is less than the threshold, then no cluster will be created or updated and the existing cluster will be known as classified. Otherwise, the algorithm will proceed to the next step for finding decision parameters to create/update new cluster(s).
- Afterward, the summation value ( $S_{ij}$ ) for each cluster distance ( $D_{ij}$ ) and the cluster's radius ( $R_j$ ) is calculated. Having the summation values, the cluster with the minimum amount of  $S_{ij}$  ( $S_a$ ) is identified as the  $C_a$  cluster. Considering the  $C_a$  cluster if  $S_a > 2.d$  ( $d$  = the given threshold), a new cluster will be formed and the algorithm will return to its initial step.
- Otherwise, the  $C_a$  cluster will be updated with its new radius equal to  $S_a/2$ .

Furthermore, Dy-NFIS equalization process starts by inserting the distorted signal and reference signal from each channel into the equalization and then specifying the value for the distance threshold ( $D_{thr}$ ) parameter in ECM.  $D_{thr}$  is a clustering parameter and is the only parameter to tune. The performance of ECM depends mostly on the choice of  $D_{thr}$  value which has predefined numbers. In terms of parameters, ECM is a distance-based clustering method that is determined by a threshold value,  $D_{thr}$ . This parameter influences how many clusters are created [40]. However, this study develops the ECM parameters of the distance threshold ( $D_{thr}$ ) to be adaptive parameters based on the reference signal. In this work, we develop the ECM parameters of the distance threshold ( $D_{thr}$ ) to be adaptive parameters based on the reference signal. ECM conducts the below steps:

- ECM depends on the Threshold value between (0, 1) to find the number of clusters.
- We used (For-Loop) from (0 to 1) with increment 0.001.
- A vector of the clustered data has been optioned.
- The suitable threshold value is the value that gets the nearest length to the reference signal.
- The threshold value that gets the nearest length to the reference signal will be chosen.

The second algorithm will be based on RLS equalization, which is based on the linear algorithm.

### 2.2.2. Linear algorithm

Furthermore, the second part of the hybrid equalization is based on the linear algorithm applied to the different adaptive filters. The implementation of an adaptive filter can be classified according to two aspects. The first is the convolution (called finite impulse response (FIR)). The second is recursion (called infinite impulse response (IIR)). FIR performs far better than IIR [78] because it settles to zero in finite time. The drawbacks are introduced using an IIR filter which is the primary motivation to use FIR filter: The IIR systems convergence tends to be slow due to the overlap between the movement of the poles and zeros [79]. The result is that even though IIR filters have fewer coefficients. Few calculations per iteration processing time to convergence may increase a net loss due to the number of iterations. The most common implementation for a linear filter is FIR, also called a transversal filter, with adjustable coefficients [80]. They are the most straightforward structures and require minimum computational multifaceted nature. The filter parameters adaptation is done by the minimization of the mean squared error (MSE) between the filter output and the reference signal based on a linear algorithm [81]. Moreover, there are different types of linear algorithms such as RLS and (LMS) algorithms. The RLS algorithm converges quicker than the LMS algorithm but has a growing complexity with the square of the number of weights making it unstable while there is a large number of weights [82]. The main function of the RLS is to update the filter weight due to the time difference. The RLS linear algorithm recursively shows the filter coefficients minimizing a weighted linear least-squares cost function of the input signals. The RLS filter converges similar optimal filter coefficients as the Wiener filter for stationary signals [50] and tracks the time variations of the process for non-stationary signals. The adaptation in the RLS optimization algorithm begins with some primary filter state and input signal successive samples utilized for the adaption of the filter coefficients [52]. First, the parameter of the optimization algorithm depends on the trial-and-error method. The parameter of the FIR filter is the number of the tap filters, the initial weight value,

the parameter of the RLS algorithm, and the forgetting factor value as shown in the flowchart. In the block, the algorithm application is optimized by the use of the symmetry of the inverse covariance matrix  $P(n)$ . This reduces whole computation numbers through two factors. The first is the use of the Filter length parameter for identifying the filter weights vector length. The second is, in the equations, the forgetting factor (0 to 1) parameter corresponding to  $\lambda$ . The corresponding RLS optimization algorithm in matrix form is  $P(n)$  [83-86]:

$$K(n) = \frac{\lambda^{-1} P(n-1) u(n)}{1 + \lambda^{-1} u^H(n) P(n-1) u(n)} \dots \dots \dots (17)$$

$$y(n) = w^T(n-1) u(n) \dots \dots \dots (18)$$

$$e(n) = d(n) - y(n) \dots \dots \dots (19)$$

$$w(n) = w(n-1) + k(n) e(n) \dots \dots \dots (20)$$

$$P(n) = \lambda^{-1} P(n-1) - \lambda^{-1} k(n) u^H(n) P(n-1) \dots \dots \dots (21)$$

In the above equation,  $\lambda^{-1}$  is the exponential weighting factor reciprocal,  $n$  is the current time index, the normalized distorted input signal is  $u(n)$  while  $d(n)$  is the normalized reference signal. In addition,  $\lambda$  refers to the forgetting factor,  $k(n)$  is the gain vector and the error signal is  $e(n)$  and  $y(n)$  indicates the filtered output. Also, the  $w(n)$  is vector of filter tap estimates while  $P(n)$  is the inverses correlation matrix [87]. The algorithm is updated based on the knowledge error signal  $e(n)$  and the normalized distorted input signal  $x(n)$ . The error signal is the variation between the filter coefficient output  $d(n)$  and the normalized reference signal  $d(n)$ . [88]

Finally, the filter coefficients are tuned perfectly and the error is minimized. An adaptive filter needs the normalized reference signal  $d(n)$  to compute the error signal  $e(n)$  for the RLS optimization algorithm. In contrast, RLS has one parameter, which is the forgetting factor. The forgetting factor is a predefined number between 0 and 1 and is used for the learning algorithm to optimize the tap coefficients of the FIR filter. The overall performance of the RLS algorithm is adjusted by the forgetting factor. The value of this parameter leads to a compromise between low maladjustment and stability on the one hand, and fast convergence rate and tracking on the other hand. In this study, the RLS algorithm will choose this specific forgetting factor parameter adaptively based on a genetic algorithm that will get better performance for the equalization process. RLS will obtain good performance after the pre-convergence. The adaptive forgetting factor is based on a Genetic algorithm and the process of using adaptive forgetting factor will be through the following steps.

- Create search space of forgetting factor value from the range [0, 1] with increment 0.1.
- Select the value from the search space randomly.
- Apply crossover to generate new value.
- Mutate the final value that will be applied as a forgetting factor.
- Apply this value of forgetting factor to RLS to start.
- Get the result of MSE by comparing the signal from RLS and the reference signal.
- Save the value of the MSE with their forgetting factor.
- If the search space is finished and then compare the MSE to get the minimum MSE.
- Fix the parameter of forgetting factor with minimum MSE and get the final output from the RLS algorithm, which is equalized signal.

Furthermore, the performance measurement in this study relies on RMSE) [89], MSE [88] and SSIM as explained in the next section

### 3. Results and discussion

This study developed hybrid equalizations to reduce Kerr nonlinear distortion in OPTICAL-CDMA over multi-mode optical fiber (MMOF). Furthermore, the performance measurement of the proposed hybrid nonlinear and linear algorithm is based on four performance measurements of RMSE [89], MSE [88], and SSIM.

- MSE is the most important criterion used to evaluate the performance of an equalization which is the average of the square error between the two signals [88]. The MSE function can be calculated from equation

$$MSE = \frac{1}{N} \sum_{i=1}^N (O_i - P_i)^2 \dots \dots \dots (22)$$

Here, n is the data length, i indicates the first index of the data matrix, distorted is the distorted signal matrix and Gaussian signal is the matrix of the designed ideal signal.

- RMSE is an estimator measuring the average of the error squares. These squares are the variation between the distorted signal and reference signal [44]. RMSE has been used in networking researches [89].

$$RMSE = \sqrt{\frac{1}{N} \sum_{i=1}^N (O_i - P_i)^2 \dots \dots \dots (23)}$$

- SSIM entails a method to measure how similar are the two signals. The SSIM index could be a quality measure of a signal compared providing that the other signal is a perfect quality in this work [90].

Here, we illustrate the achieved outcomes of hybrid equalization techniques in the Optical-CDMA over MMOF based on nonlinear and linear digital signal processing (DSP) for high-capacity optical communication networks. In the hybrid equalization, we have run the system based on adaptive parameters. These results have been compared to get the best results. Furthermore, as mentioned above, the performance measurement results in this study depend on MSE [88], RMSE [89], and SSI illustrated in Figure 8, Figure 9, Figure 10, and Figure 11 and Table 1, Table 2, and Table 3.

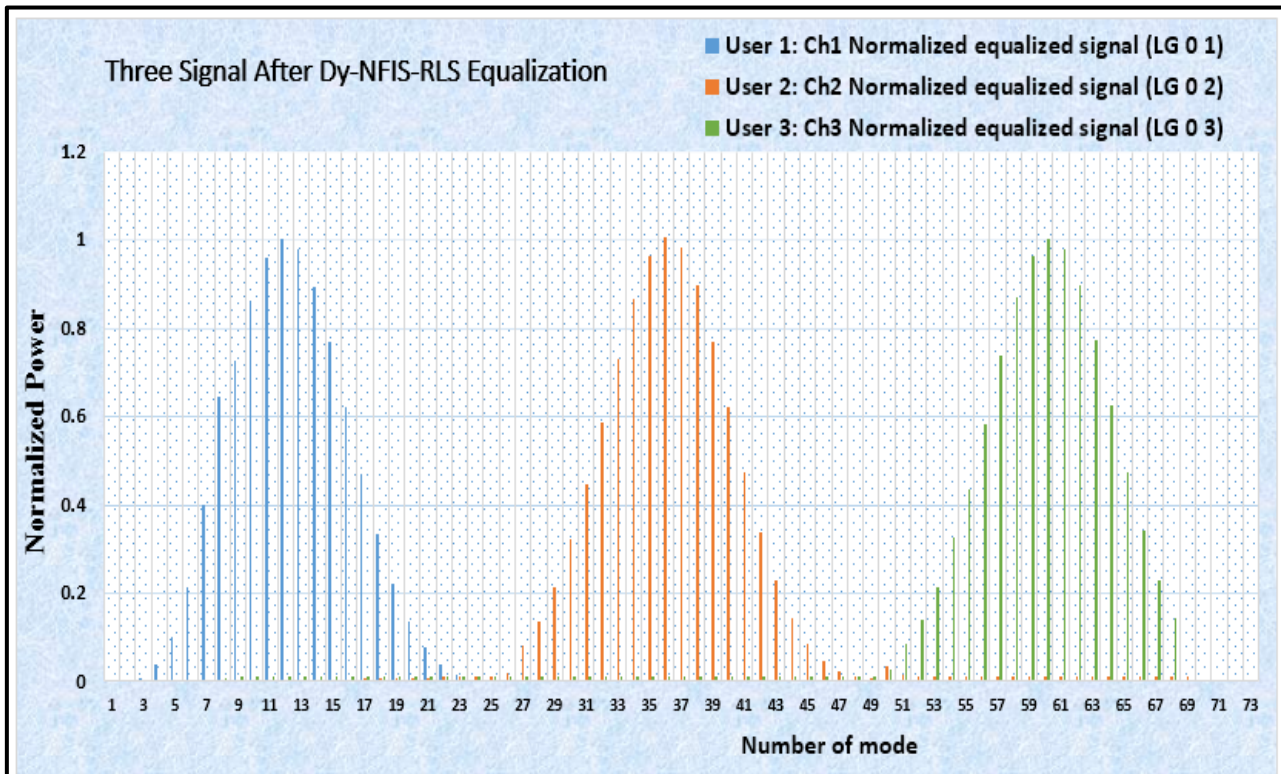


Figure 8. The representations of the three equalized signals at the receiver after a hybrid algorithm



The parameters of the hybrid equalizations are ECM parameters of the adaptive distance threshold (A-Dthr) in Dy-NFIS and the parameters of RLS based on (adaptive forgetting factor (A-FF)) are important for the results. In this study, the setting of the parameters based on adaptive parameters. These parameters are adaptive distance threshold (A-Dthr) and adaptive forgetting factor (A-FF)) value for all the users. Then, the distorted signals are removed. Settings the parameters depend on the adaptive parameter as mentioned before; the values of the adaptive distance threshold (A-Dthr) of the Dy-NFIS algorithm are between 0 to 1. The parameters of the RLS algorithm are based on the adaptive parameters which are adaptive forgetting factors (A-FF) that are between (0 to 1). The adaptive parameters that have been chosen for the hybrid equalizations are (Adaptive distance threshold (A-Dthr), and Adaptive forgetting factor (A-AF)). Form Figure 9 shows that the parameters for Ch1: User 1 are site to (0.066, and 0.1). In Ch2, User 2 (0.018, and 0.6) are 0.022, and 0.2 while for Ch3, User 3, the results of the three channels are represented in Figure 8 that show there are no interferences between the three signals.

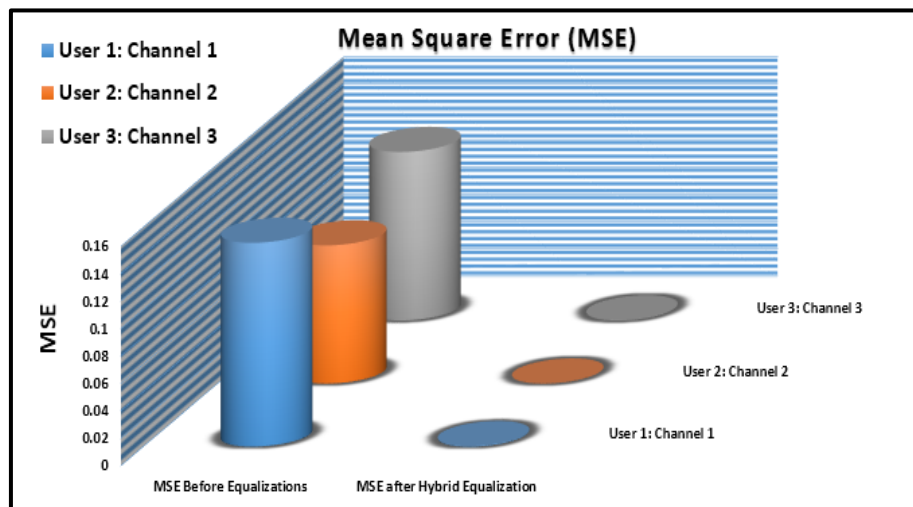


Figure 9. The results of MSE before and after a hybrid equalization.

Figure 9 and Table 1 show that for Ch1, User 1, the parameters are (A-Dthr 0.066, and AF-F 0.1) and the results of MSE before the hybrid equalization are 0.1485 and after hybrid equalization become 4.49E-04. With Ch2, User 2, the parameters are (A-Dthr 0.018, and 0.6). The results of MSE before the hybrid equalization are 0.1007 and following a hybrid equalization, it is 4.89E-05. For Ch3, User 3, the parameters are A-Dthr 0.022, and AF-F 0.2, and the result of MSE of the pre- hybrid equalization is 0.1228 and post hybrid equalization is 1.59E-04. The standard MSE value is about zero, as the hybrid equalization for three equalized channels is almost near to zero. Moreover, Figure 10 and Table 2 above illustrate the results of RMSE for three channels. In Ch1, User 1, the parameters are A-Dthr 0.066, and AF-F 0.1 with a value of RMSE before the hybrid equalization (0.3854). It becomes 0.0212 after the hybrid equalization. With Ch2, User 2, the parameters are A-Dthr 0.018, and 0.6 with 0.3173. RMSE before and after the hybrid equalization is 0.3173 and 0.0070 respectively. For Ch3, User 3, the parameters are A-Dthr 0.022, and AF-F 0.2 and (0.3504) RMSE before the hybrid equalization and (0.0126) after the hybrid equalization is r. The standard RMSE value is nearly zero for three equalized channels is almost near to zero.

Table 2. The results of MSE before and after a hybrid equalization

Channels	MSE results before a hybrid equalization	MSE results after a hybrid equalization
Channel 1	0.1485	4.49E-04
Channel 2	0.1007	4.89E-05
Channel 3	0.1228	1.59E-04

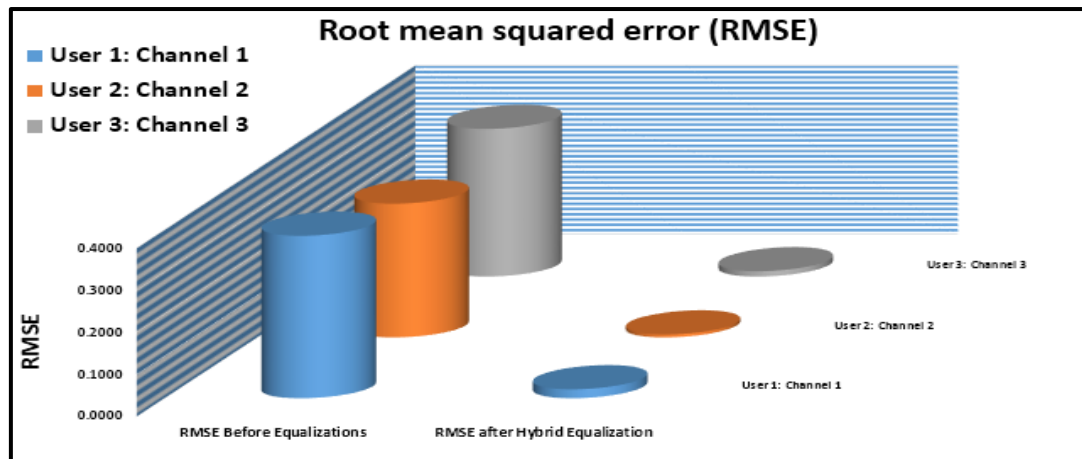


Figure 10. The results of RMSE before and after a hybrid equalization

Table 3. The results of RMSE before and after a hybrid equalization

Channels	RMSE results before Equalization	RMSE results after a hybrid Equalization
Channel 1	0.3854	0.0212
Channel 2	0.3173	0.0070
Channel 3	0.3504	0.0126

Furthermore, From Figure 11 and Table 4 above illustrate the results of Structural Similarity index for three channels. In Ch1, User 1, the parameters are A-Dthr 0.066, and AF-F 0.1 and the results of SSIM before the hybrid equalization is 0.1407 and after hybrid equalization 0.9650 as shown in Figure 8. Also, the representations of the Ch1, User 1, the equalized signal is distorted signals that have been eliminated. With Ch2, User 2, the parameters are A-Dthr 0.018, and 0.6 and the results of SSIM before the hybrid equalization is 0.2090 and turned to be 0.9014 following the hybrid equalization as shown in Figure 8. The Ch2, User 2, the equalized signal is showed that distorted has been eliminated. For Ch3: User 3: the parameters are (A-Dthr 0.022, and AF-F 0.2), and the results of SSIM before the hybrid equalization is (0.0577) and after hybrid equalization is (0.7864). Figure 8 shows the representations of the Ch3, User 3, of the equalized signal that is distorted eliminated. SSIM index is a quality measure of one of the signals being compared provided the other signal is regarded as of perfect quality in this research. The standard SSIM value is to be near to one, which can see from the results above that after using hybrid equalization for three equalized channels is almost near to one. The distortions signal and the noise from the signals have been eliminated. In the next section we will explain the evaluation study.

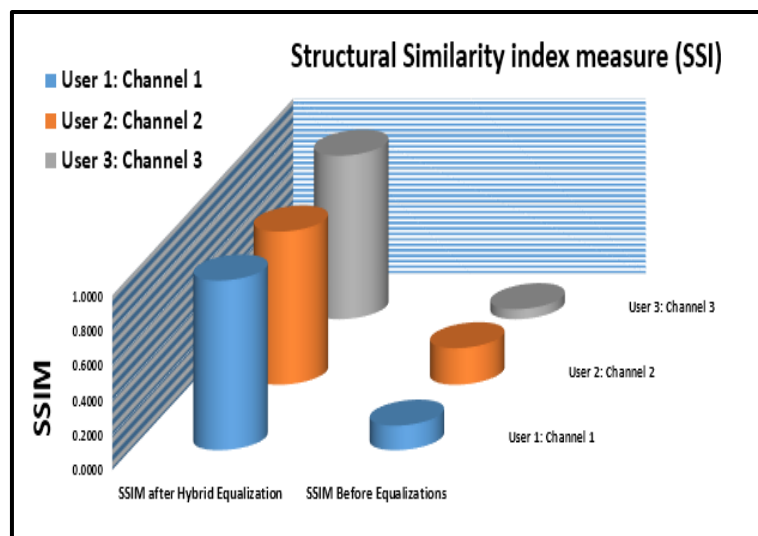


Figure 11. The results of the Structural Similarity Index (SSIM) before and after a hybrid equalization.

Table 4. The results of the Structural Similarity Index (SSIM) before and after a hybrid equalization

Channels	SSIM results before Equalizations	SSIM results after a hybrid Equalization
Channel 1	0.1407	0.9650
Channel 2	0.2090	0.9014
Channel 3	0.0577	0.7864

#### 4. Compression study

In this study, the equalization for OPTICAL-CDMA over MMOF based on hybrid nonlinear and linear equalization will be evaluated by comparing it with the previous equalization-based MSE, RMSE, and SSIM measurements. We reviewed different literature reviews and, this study compares Dy-NFIS-RLS algorithms with RLS algorithm. Figure 12 (a, b, and c) shows the three distorted signals before equalization and the three equalized signals after RLS equalizations. The three equalized signals appear after Dy-NFIS-RLS equalizations. We can see that the DyNFIS-RLS equalization can reduce the noise in the signal when compared to RLS equalization.

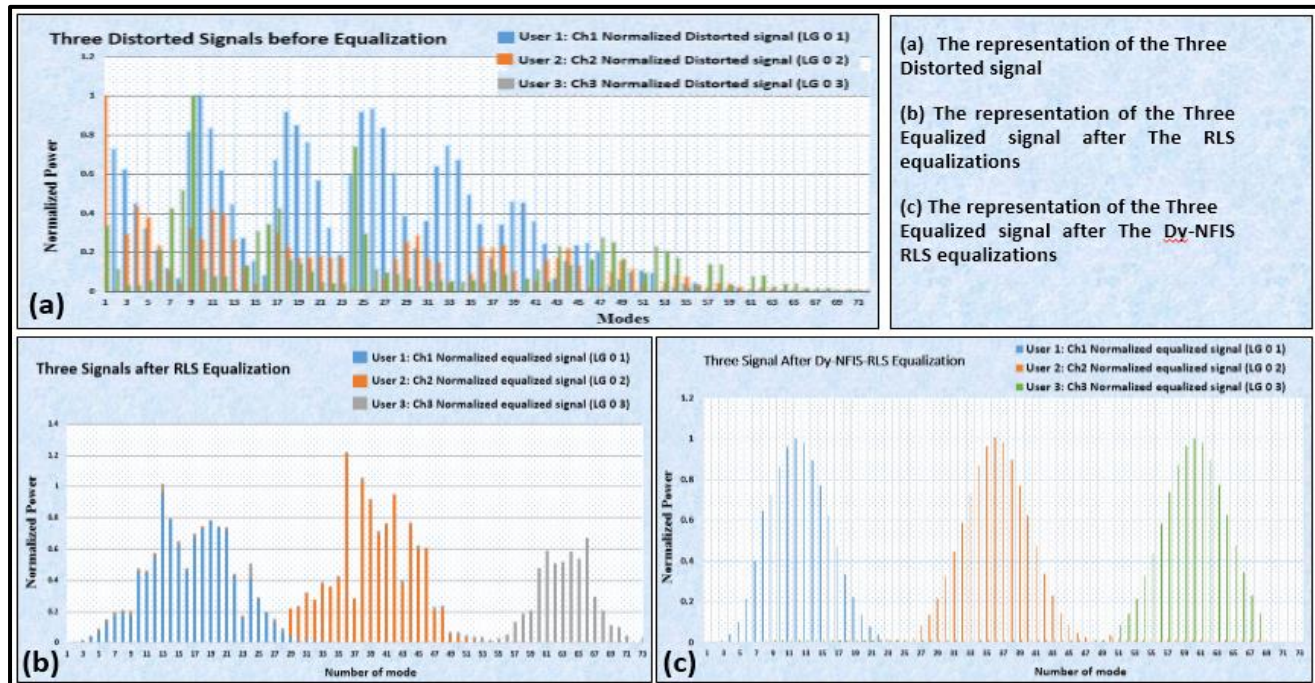


Figure 12. (a) the representation of three distorted signals pre-and-post a hybrid equalization signal after RLS equalizations (c) the representation of three equalized signals after Dy-NFIS-RLS equalizations

Moreover, Table 4 and Figure 13 represent the compression results based on the MSE of three distorted signals of the three channels before equalization. For User 1: CH1 the results of MSE are 0.1485 while User 2: CH2 and User 3: CH3 are 0.1007 and 0.1228 respectively. For User 1, CH1 and User 2, CH2, the MSE results after RLS equalizations are 0.0416 and 0.0404 respectively, However, the third is 0.0352 based on RLS parameters which are 5 tap filters for each of the three channels, (0.7 forgetting factor value) for channel 1, (0.4 forgetting factor value) for channel 2, and the forgetting factor value is 0.2 for channel 3. The results of MSE after a hybrid Dy-NFIS-RLS equalizations for Ch1, User 1, the parameters are A-Dthr 0.066, and AF-F 0.1 and the results of MSE after hybrid equalization  $4.49 \times 10^{-4}$ . With Ch2, User 2, the parameters are A-Dthr 0.018, and 0.6, the results of MSE after hybrid equalization is  $4.89 \times 10^{-5}$ . For Ch3, User 3, the parameters are A-Dthr 0.022, and AF-F 0.2, and the results of MSE after hybrid equalization is  $1.59 \times 10^{-4}$ . The standard MSE value is approximately zero and the hybrid equalizations have been reduced the noise. In addition, the distorted nonlinear and the noise in the three channels are successful.

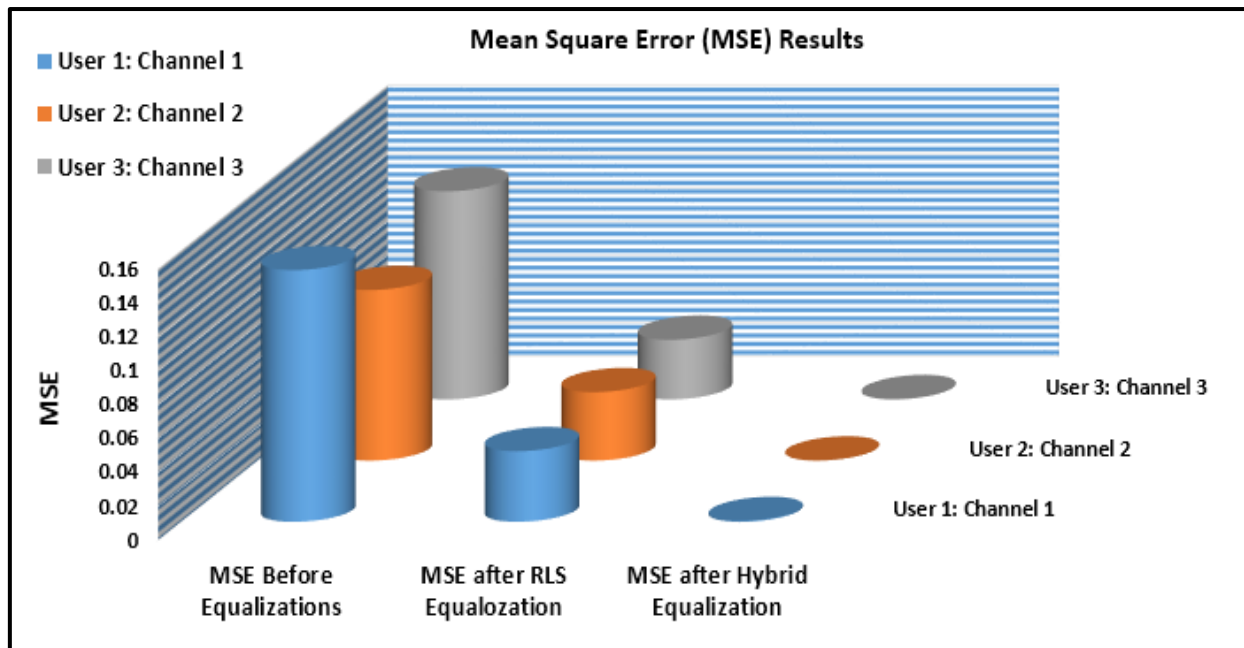


Figure 13. The results of MSE of the three distorted signals before equalization, the three equalized signals after RLS equalizations, and the three equalized signals after Dy-NFIS- RLS equalizations.

Table 5. The results of MSE of the three distorted signals before equalization, the three equalized signals after RLS equalization, and the three equalized signals after Dy-NFIS- RLS equalizations

Channels	MSE results before a hybrid equalization	MSE results after RLS equalization	MSE results after Dy-NFIS- RLS equalization
User 1 :Ch1	0.1485	0.0417	4.49E-04
User 1 :Ch1	0.1006	0.0404	4.89E-05
User 1 :Ch1	0.1227	0.0352	1.59E-04

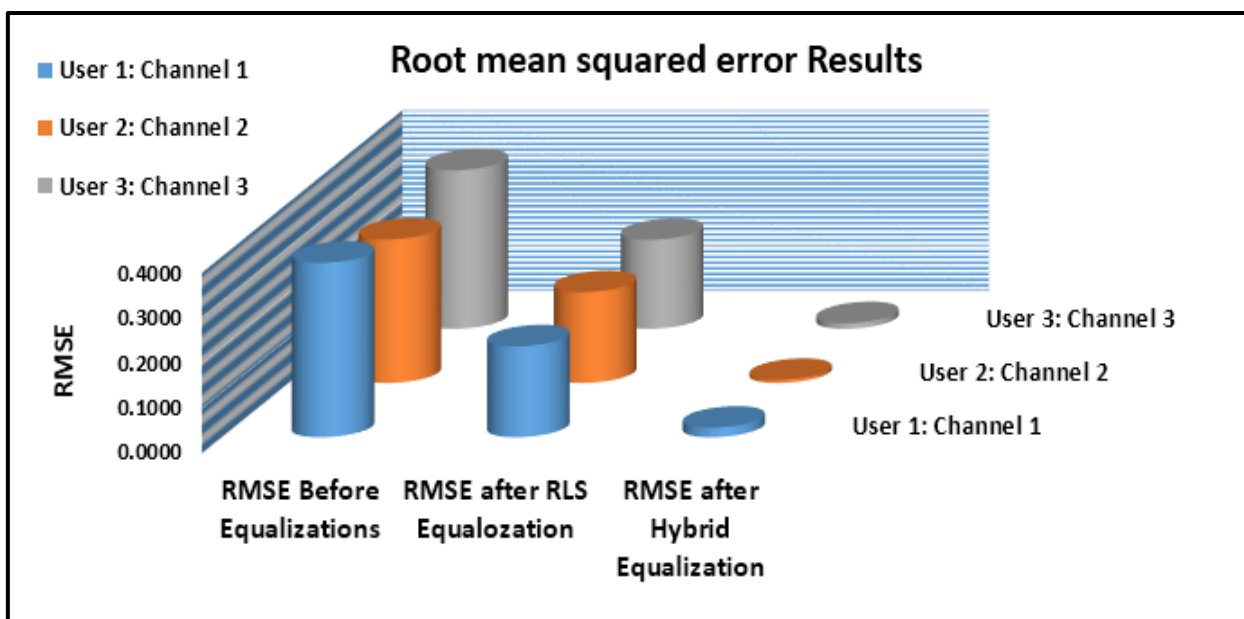


Figure 14. The results of RMSE of the three distorted signals before equalization, the three equalized signals after RLS equalizations, and the three equalized signals after Dy-NFIS- RLS equalizations.



Table 6. The results of RMSE of the three distorted signals before equalization, the three equalized signals after RLS equalization, and the three equalized signals after Dy-NFIS- RLS equalizations

Channels	RMSE results before a hybrid equalization	RMSE results after RLS equalization	RMSE results after Dy-NFIS-RLS equalization
User 1 :Ch1	0.3854	0.2010	0.0212
User 1 :Ch1	0.3173	0.2010	0.0070
User 1 :Ch1	0.3504	0.1968	0.0126

Table 6 and Figure 14 show that RMSE results for the distorted signal for User 1, CH1, is 0.3854 while it is respective 0.3173, and 0.3504 for User 2: CH2 and User 3: CH3. RMSE results for the equalized signal after RLS equalization for User 1, CH1, User 2, CH2 and User 3, CH3 are 0.2010, 0.2010, and 0.1968 based on 5 tap filters for all the channels and the forgetting factor value for the User, CH1 is 0.7 the User 2, CH2 0.4 and the User 3, CH3 0.2. The equalized signals of the first channel are 0.2010 and the second shows 0.2010 while it seems to be 0.1968 based on RLS 5 tap filter, 0.7 for all the channels. The forgetting value for the first channel is 0.7 the second 0.4 and the third 0.2. The three equalized signals after hybrid Dy-NFIS- RLS equalizations are for Ch1: User 1: the parameters are (A-Dthr 0.066, and AF-F 0.1) and the results of MSE after hybrid equalization become (4.49E-04). With Ch2, User 2, the parameters are A-Dthr 0.018, and 0.6. The MSE after hybrid equalization is 4.89E-05. For Ch3, User 3, the parameters are A-Dthr 0.022, and AF-F 0.2, and MSE after hybrid equalization is 1.59E-04. The standard RMSE value is about zero following the use of the hybrid equalization, the distorted nonlinear, and the noise in the three channels become proximately zero, which is lower than that of RLS equalization.

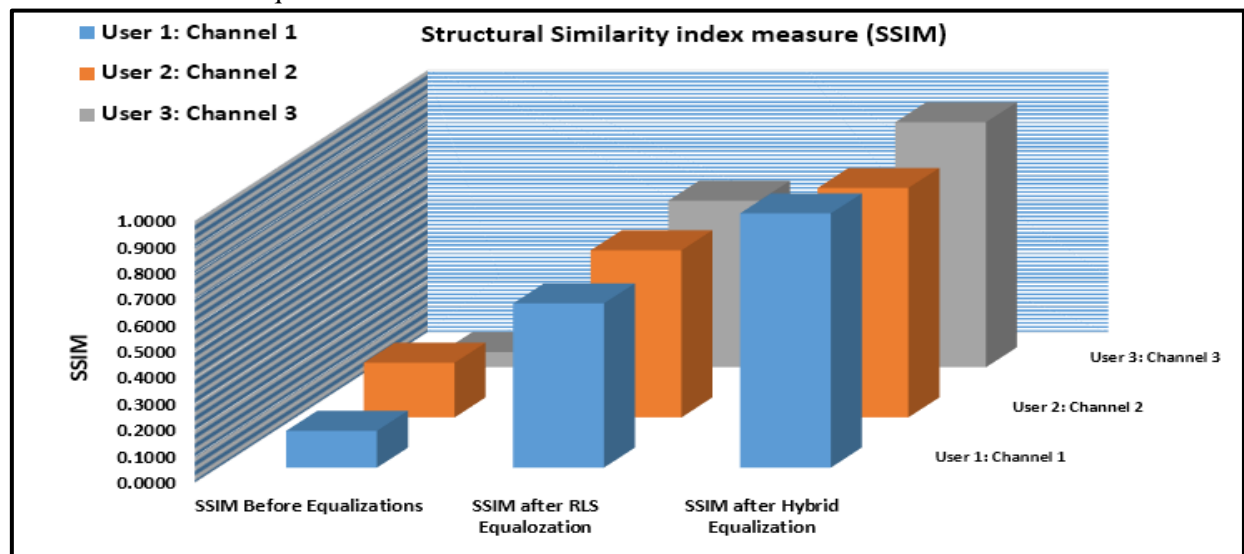


Figure 15. The results of SSIM of the three distorted signals before equalization and the three equalized signals after RLS equalizations and the three equalized signals after Dy-NFIS- RLS equalizations.

Table 7. The results of SSIM of the three distorted signals before equalization and the three equalized signals after RLS equalization and the three equalized signals after Dy-NFIS- RLS equalizations.

Channels	SSIM results before a hybrid equalization	SSIM results after RLS equalization	SSIM results after Dy-NFIS-RLS equalization
User 1 :Ch1	0.1407	0.6272	0.9710
User 1 :Ch1	0.2090	0.6384	0.8764
User 1 :Ch1	0.0577	0.6361	0.9358

Table 7 and Figure 15 show the SSIM results of three distorted signals, In User 1, CH1, User 2, CH2, and User 3, CH3 are 0.1407, 0.2090, and 0.0577. SSIM results of the three equalized signals after RLS equalizations for



User 1, CH1, User 2, CH2, and User 3, CH3 are 0.6272, 0.6384, and 0.6361. When the tap filter of the RLS parameter is 5 for each of the three channels, the forgetting factor values for User 1, CH1; User 2: CH2 is 0.7, and 0.4 while User 3, CH3, the forgetting factor value is 0.2. The three equalized signals after hybrid Dy-NFIS-RLS equalizations in Ch1, User 1, the parameters are A-Dthr 0.066, and AF-F 0.1 and the results of SSIM following the hybrid equalization 0.9650. In Ch1, User, the equalized signal shows that the distorted signal has been eliminated. With Ch2, User 2, the parameters are A-Dthr 0.018, and 0.6) and the results of SSIM after hybrid equalization is 0.9014. As shown in Figure 8, the representations of the Ch2, User 2, the equalized signal is distorted and has been eliminated. For Ch3, User 3, the parameters are A-Dthr 0.022 and AF-F 0.2, and the results of SSIM after hybrid equalization is 0.7864. In Ch3, User 3, the equalized signal is distorted eliminated. SSIM index is a quality measure of one of the signals being compared provided that the other signal is regarded as of perfect quality in this research. The standard SSIM value is about one. The results above show that after using hybrid equalization for the three equalized channels is almost near to one. The distortions signal and the noise from the signals have been eliminated.

## 5. Conclusion

Today, the methods of creation, control, manipulation, and measurement of ultrashort optical pulses and certain waveforms are very significant in many scientific fields, such as ultrahigh-speed optical communications. Machine learning plays an important role in the optical communication system to manipulate the distortion in the quality of signals. However, during the propagation of data over the MMOF based on OPTICAL-CDMA, an inevitable encountered issue is pulse dispersion, nonlinearity, and MAI due to mode coupling. Moreover, pulse dispersion, nonlinearity, and MAI are important for the evaluation of the performance of high-speed MMOF communication systems based on the OPTICAL-CDMA. This work developed a hybrid algorithm according to a nonlinear algorithm (Dynamic evolving neural fuzzy inference (Dy-NFIS)) and a linear algorithm (Recursive least squares (RLS)) equalization for ZCC code in OPTICAL-CDMA over MMOF that have been successfully totally reduced. Then, the nonlinear is distorted and the noise is reduced. The parameters of the hybrid algorithm have been applied based on the adaptive parameters and the best parameters that have been chosen to enhance the performance of hybrid equalizations. The performance measurement is evaluated according to RMSE, MSE, and SSIM with RLS equalizations.

## References

- [1] O. Lopez, N. Chiodo, F. Stefani, F. Wiotte, N. Quintin, A. Bercy, C. Chardonnet, G. Santarelli, P.-E. Pottie, and A. Amy-Klein, "Cascaded optical link on a telecommunication fiber network for ultra-stable frequency dissemination," in *Slow Light, Fast Light, and Opto-Atomic Precision Metrology VIII*, International Society for Optics and Photonic's, 2015, vol. 9378, p. 937823.
- [2] G. Li, N. Bai, N. Zhao, and C. Xia, "Space-division multiplexing: the next frontier in optical communication," *Advances in Optics and Photonics*, vol. 6, no. 4, pp. 413-487, 2014.
- [3] X. Guo, Q. Wang, X. Li, L. Zhou, L. Fang, A. Wonfor, J. Wei, J. von Lindeiner, R. Pentty, and I. White, "First demonstration of OFDM ECDMA for low cost optical access networks," *Optics letters*, vol. 40, no. 10, pp. 2353-2356, 2015.
- [4] D. Richardson, J. Fini, and L. Nelson, "Space-division multiplexing in optical fibres," *Nature Photonics*, vol. 7, no. 5, p. 354, 2013.
- [5] S. Chebaane, H. Fathallah, H. Seleem, and M. Machhout, "Trenched raised cosine FMF for differential mode delay management in next generation optical networks," *Optics Communications*, vol. 408, pp. 15-20, 2018.
- [6] D. Qian, M.-F. Huang, E. Ip, Y.-K. Huang, Y. Shao, J. Hu, and T. Wang, "101.7-Tb/s (370× 294-Gb/s) PDM-128QAM-OFDM transmission over 3× 55-km SSMF using pilot-based phase noise mitigation," in *National Fiber Optic Engineers Conference*, p. PDPB5:2011.

- 
- [7] A.M. Kabbour, H.A. Fadhil, A. Amphawan, S.A. Aljunid, and M.K. AlMustafa, "Comparison of Single Mode Fiber and Multimode Fiber in Deployment of SCM-OCDMA in Local Area Network," *Key Engineering Materials*, Vol. 594, pp. 1037-1040, 2014.
  - [8] H. Mrabet and S. Mthali, "Performance enhancement of OCDMA systems for LAN consideration," *IET Optoelectronics*, vol. 10, no. 6, pp. 199-204, 2016.
  - [9] H. Mrabet, I. Dayoub, R. Attia, and W. Hamouda, "Wavelength and beam launching effects on silica optical fiber in local area networks," *Optics Communications*, vol. 283, no. 21, pp. 4234-4241, 2010.
  - [10] C. Tatkeu, D. Loum, I. Dayoub, M. Heddebaut, and J. Rouvaen, "Theoretical and Experimental Performances Evaluation of a New Multiple Access Technique for Optical Fibers," *International Journal of Information Engineering*, vol. 2, pp. 129-137, 2012.
  - [11] C.-T. Yen and W.-B. Chen, "A Study of Dispersion Compensation of Polarization Multiplexing-Based OFDM-OCDMA for Radio-over-Fiber Transmissions," *Sensors*, vol. 16, no. 9, p. 1440, 2016.
  - [12] S.M.S.S. Kharazi, G.A. Mahdiraji, R.K.Z. Sahbudin, A.F. Abas, and S.B.A. Anas, "Effects of fiber dispersion on the performance of optical CDMA systems," pp.311-320, 2012.
  - [13] Z.A. Almatroudi, A. Ragheb, A. Bentrchia, and H. Fathallah, "Spectral phase coding based LR-PON," in *Innovations in Information Technology (IIT), 2015 11th International Conference on*, pp. 7-10: IEEE 2015.
  - [14] M. de Paula Marques, F.R. Durand, and T. Abrão, "WDM/OCDM energy-efficient networks based on heuristic ant colony optimization," *IEEE Systems Journal*, vol. 10, no. 4, pp. 1482-1493, 2016.
  - [15] A.M. Kabbour, A. Amphawan, H.A. Fadhil, and S.A. Aljunid, "Selective mode excitation in SCM-OCDMA," in *Photonics (ICP), 2013 IEEE 4th International Conference on*, 2013, pp. 200-202: IEEE.
  - [16] H. Fathallah, A. Bentrchia, and H. Seleem, "Efficient interference cancellation detector for asynchronous upstream optical code division multiple access-passive optical network with mixed Poisson–Gaussian noise," *IET Communications*, vol. 8, no. 13, pp. 2393-2403, 2014.
  - [17] P. Singh, M. Kumar, and A. Sharma, "Design and Performance investigation of multiuser OCDMA network," *International Journal of Scientific & Engineering Research*, vol. 4, no. 7, pp. 2549-2552, 2013.
  - [18] P. Sharma, S. Kaushal, A.S. Sharma, and J.S. Malhotra, "Link length augmentation of optically coded multi-user network by using Electronic Equalization Technique," in *Engineering and Computational Sciences (RAECS), 2014 Recent Advances in*, 2014, pp. 1-5: IEEE.
  - [19] M.S. Ahmed and I. Glesk, "Recent advances in all-optical signal processing for performance enhancements of OCDMA interconnects," 2016.
  - [20] D. Chen, J. Wang, J. Jin, H. Lu, and L. Feng, "A CDMA system implementation with dimming control for visible light communication," *Optics Communications*, vol. 412, pp. 172-177, 2018.
  - [21] J. Lian and M. Brandt-Pearce, "MIMO signal processing for multiuser VLC systems," in *Photonics Society Summer Topical Meeting Series (SUM), 2016 IEEE*, 2016, pp. 60-61: IEEE.
  - [22] G. Kaur and S. Singh, "Review on Optical Code Division Multiple Access Systems," *International Journal of Engineering Sciences, Jan*, vol. 17, 2016.
  - [23] F. Akhoundi, M.V. Jamali, N.B. Hassan, H. Beyranvand, A. Minoofar, and J.A. Salehi, "Cellular underwater wireless optical CDMA network: Potentials and challenges," *IEEE Access*, vol. 4, pp. 4254-4268, 2016.
  - [24] J. Lian and M. Brandt-Pearce, "Distributed power allocation for multiuser MISO indoor visible light communications," in *Global Communications Conference (GLOBECOM), 2015 IEEE*, 2015, pp. 1-7: IEEE.
  - [25] A.A. Saed, M. Yasir, S.-W. Ho, and C.W. Sung, "Coding for uncoordinated multiple access in visible light positioning systems," in *Signal Processing and Communication Systems (ICSPCS), 2016 10th International Conference on*, 2016, pp. 1-7: IEEE.
  - [26] H.T.S. Al-Rikabi, *Enhancement of the MIMO-OFDM Technologies*. California State University, Fullerton, 2013.
-

- 
- [27] N. Eiselt, H. Griesser, J. Wei, R. Hohenleitner, A. Dochhan, M. Ortsiefer, M.H. Eiselt, C. Neumeyr, J.J.V. Olmos, and I.T. Monroy, "Experimental Demonstration of 84 Gb/s PAM-4 Over up to 1.6 km SSMF Using a 20-GHz VCSEL at 1525 nm," *Journal of Lightwave Technology*, vol. 35, no. 8, pp. 1342-1349, 2017.
  - [28] T. Xia, C. Guo, and S. He, "Impact of ADC bandwidth and clipping ratio on COF-PON systems based on spatial coding and subcarrier multiplexing," in *Photonics and Optoelectronics (SOPO), 2011 Symposium on*, 2011, pp. 1-4: IEEE.
  - [29] C. Yang, Y. Wang, Y. Wang, X. Huang, and N. Chi, "Demonstration of high-speed multi-user multi-carrier CDMA visible light communication," *Optics Communications*, vol. 336, pp. 269-272, 2015.
  - [30] M.Z. Farooqui and P. Saengudomlert, "Transmit power reduction through subcarrier selection for MC-CDMA-based indoor optical wireless communications with IM/DD," *EURASIP Journal on Wireless Communications and Networking*, vol. 2013, no. 1, p. 138, 2013.
  - [31] S. Sahoo, U. Dash, S. Parashar, and S. Ali, "Frequency and temperature dependent electrical characteristics of CaTiO<sub>3</sub> nano-ceramic prepared by high-energy ball milling," *Journal of Advanced Ceramics*, vol. 2, no. 3, pp. 291-300, 2013.
  - [32] D. Patel, V.K. Singh, and U. Dalal, "Analysis of second order harmonic distortion due to transmitter non-linearity and chromatic and modal dispersion of optical OFDM SSB modulated signals in SMF-MMF fiber links," *Optics Communications*, vol. 383, pp. 294-303, 2017.
  - [33] N.A.H. Hala A. Naman, Mohand Lokman Al-dabag, Haider Th.Salim Alrikabi, "Encryption System for Hiding Information Based on Internet of Things," *International Journal of Interactive Mobile Technologies (iJIM)*, vol. 15, no. 2, 2021.
  - [34] M.B. Shemirani and J.M. Kahn, "Higher-order modal dispersion in graded-index multimode fiber," *Journal of Lightwave Technology*, vol. 27, no. 23, pp. 5461-5468, 2009.
  - [35] S.P. Singh and N. Singh, "Nonlinear effects in optical fibers: origin, management and applications," *Progress In Electromagnetics Research*, vol. 73, pp. 249-275, 2007.
  - [36] J. Mohammed, "A study on the suitability of genetic algorithm for adaptive channel equalization," *International journal of electrical and computer engineering*, vol. 2, no. 3, p. 285, 2012.
  - [37] R. Salah Khairy, A. Hussein, H. Salim ALRikabi, "The Detection of Counterfeit Banknotes Using Ensemble Learning Techniques of AdaBoost and Voting," *International Journal of Intelligent Engineering and Systems*, vol. 14, no. 1, pp. 326-339, 2021.
  - [38] Y.-C. Hwang and Q. Song, "Dynamic neural fuzzy inference system," in *International Conference on Neural Information Processing*, 2008, pp. 1245-1250: Springer.
  - [39] Q. Song and N. Kasabov, "ECM-A novel on-line, evolving clustering method and its applications," *Foundations of cognitive science*, pp. 631-682, 2001.
  - [40] N.K. Kasabov and Q. Song, "DENFIS: dynamic evolving neural-fuzzy inference system and its application for time-series prediction," *IEEE transactions on Fuzzy Systems*, vol. 10, no. 2, pp. 144-154, 2002.
  - [41] S. Soltic, S. Pang, N. Kasabov, S. Worner, and L. Peacock, "Dynamic neuro-fuzzy inference and statistical models for risk analysis of pest insect establishment," in *International Conference on Neural Information Processing*, 2004, pp. 971-976: Springer.
  - [42] A. Talei, L. Chua, and C. Quek, "Dynamic Evolving Neural-Fuzzy Inference System for Rainfall-Runoff (RR) Modelling," in *Proceedings of the 34th World Congress of the International Association for Hydro-Environment Research and Engineering: 33rd Hydrology and Water Resources Symposium and 10th Conference on Hydraulics in Water Engineering*, 2011, p. 1514: Engineers Australia.
  - [43] A. Almomani, B. Gupta, T.-c. Wan, A. Altaher, and S. Manickam, "Phishing dynamic evolving neural fuzzy framework for online detection zero-day phishing email," *arXiv preprint arXiv:1302.0629*, 2013.
  - [44] S. Heddami, "Modelling hourly dissolved oxygen concentration (DO) using dynamic evolving neural-fuzzy inference system (DENFIS)-based approach: case study of Klamath River at Miller Island Boat Ramp, OR, USA," *Environmental Science and Pollution Research*, vol. 21, no. 15, pp. 9212-9227, 2014.
-

- 
- [45] M.O. Elish, "A comparative study of fault density prediction in aspect-oriented systems using MLP, RBF, KNN, RT, DENFIS and SVR models," *Artificial Intelligence Review*, vol. 42, no. 4, pp. 695-703, 2014.
  - [46] R.M. Saad, A. Almomani, A. Altaher, B. Gupta, and S. Manickam, "ICMPv6 flood attack detection using DENFIS algorithms," *Indian Journal of Science and Technology*, vol. 7, no. 2, p. 168, 2014.
  - [47] A. Almomani, A. Obeidat, K. Alsaedi, M.A.-H. Obaida, and M. Al-Betar, "Spam e-mail filtering using ECOS algorithms," *Indian Journal of Science and Technology*, vol. 8, no. S9, pp. 260-272, 2015.
  - [48] C.T. Kwin, A. Talei, S. Alaghmand, and L.H. Chua, "Rainfall-runoff modeling using dynamic evolving neural fuzzy inference system with online learning," *Procedia engineering*, vol. 154, pp. 1103-1109, 2016.
  - [49] G. Piscopo, "Dynamic evolving neuro fuzzy inference system for mortality prediction," *Int. J. Eng. Res. Appl.*, vol. 7, no. 3, pp. 26-29, 2017.
  - [50] H. Malani, "System identification through RLS adaptive filters," *matrix*, vol. 1, p. 1, 2012.
  - [51] J. Dhiman, S. Ahmad, and K. Gulia, "Comparison between Adaptive filter Algorithms (LMS, NLMS and RLS)," *International Journal of Science, Engineering and Technology Research (IJSETR)*, vol. 2, no. 5, pp. 1100-1103, 2013.
  - [52] S. Dixit and D. Nagaria, "LMS adaptive filters for Noise Cancellation: A Review," *International Journal of Electrical and Computer Engineering (IJECE)*, vol. 7, no. 5, pp. 2520-2529, 2017.
  - [53] H.T. Alrikabi, A.H.M. Alaidi, A.S. Abdalrada, and F.T. Abed, "Analysis the Efficient Energy Prediction for 5G Wireless Communication Technologies," *International Journal of Emerging Technologies in Learning (iJET)*, vol. 14, no. 08, pp. 23-37, 2019.
  - [54] A.A.-D. Alaam Ghazi Ahmed M. Fakhrudeen Mohammed Nasih Ismael, Sara Alshwani, "SDM over hybrid FSO link under different weather conditions and fth based on electrical equalization" *International Journal of Civil Engineering and Technology*, vol. 10, no. 1, pp. 1396-1406, 2019.
  - [55] M. Release, "The mathworks," *Inc., Natick, Massachusetts, United States*, vol. 488, 2013.
  - [56] A.M.F. S. A. Aljunid and Syed Zulkarnain Syed Idrus Sara Alshwani, Mohammed Nasih Ismael, Aras Al-Dawoodi, Alaam Ghazi, "Hermite-gaussian mode in spatial division multiplexing over fso system under different weather condition based on linear gaussian filter," *International Journal of Mechanical Engineering and Technology (IJMET)*, vol. 10, no. 1, pp. 1095-1105, 2019/2/2.
  - [57] A. Ghatak and K. Thyagarajan, *An introduction to fiber optics*. Cambridge university press, 1998.
  - [58] I. Bala and V. Rana, "Gaussian approximation analysis of ZCC code for multimedia optical CDMA applications," in *2009 11th International Conference on Transparent Optical Networks*, 2009, pp. 1-4: IEEE.
  - [59] M. Anuar, S. Aljunid, N. Saad, A. Mohammed, and E. Babekir, "Development of a zero cross-correlation code for spectralamplitude coding optical code division multiple access (OCDMA)," *Int. J. Comput. Sci. Network Security*, vol. 6, pp. 180-184, 2006.
  - [60] C. Rashidi, S. Aljunid, and F. Ghani, "Design of a new class of codes with zero in phase cross correlation for spectral amplitude coding," *IJCSNS Int. J. Comput. Sci. Netw. Secur.*, vol. 11, pp. 237-242, 2011.
  - [61] N.A. Ahmad, M. Junita, S. Aljunid, C. Rashidi, and R. Endut, "Analysis of hybrid subcarrier multiplexing of OCDMA based on single photodiode detection," in *EPJ Web of Conferences*, 2017, vol. 162, p. 01028: EDP Sciences.
  - [62] M. Anuar, S. Aljunid, A. Arief, and N. Saad, "LED spectrum slicing for ZCC SAC-OCDMA coding system," in *7th International Symposium on High-capacity Optical Networks and Enabling Technologies*, 2010, pp. 128-132: IEEE.
  - [63] A. Kang and V. Sharma, "Pulse shape filtering in wireless communication-a critical analysis," *International Journal of Advanced Computer Science and Applications*, vol. 2, no. 3, 2011.
  - [64] H. Wang, A.I. Latkin, S. Boscolo, P. Harper, and S.K. Turitsyn, "Generation of triangular-shaped optical pulses in normally dispersive fibre," *Journal of optics*, vol. 12, no. 3, p. 035205, 2010.
-

- 
- [65] N.D.A. Sorin Pohoată, Adrian Popa, "An approximation of gaussian pulses," *International Conference on Pervasive and Embedded Computing and Communication Systems*, 2011.
  - [66] A. Fareed, A. Amphawan, Y. Fazea, M.S. Sajat, and S.C. Chit, "Channel Impulse Response Equalization based on Genetic Algorithm in Mode Division Multiplexing," *Journal of Telecommunication, Electronic and Computer Engineering (JTEC)*, vol. 10, no. 2-4, pp. 149-154, 2018.
  - [67] A. Noori, A. Amphawan, A. Ghazi, and S.A. Ghazi, "Dynamic evolving neural fuzzy inference system equalization scheme in mode division multiplexer for optical fiber transmission," *Bulletin of Electrical Engineering and Informatics*, vol. 8, no. 1, pp. 127-135, 2019.
  - [68] S. Pohoata, A. Popa, and N.D. Alexandru, "Generation of Quasi-Gaussian Pulses Based on Correlation Techniques," *Advances in Electrical and Computer Engineering*, vol. 12, no. 1, pp. 71-76, 2012.
  - [69] L.-X. Wang, "Adaptive fuzzy systems and control," *Design and stability analysis*, 1994.
  - [70] T. Takagi and M. Sugeno, "Fuzzy identification of systems and its applications to modeling and control," *IEEE transactions on systems, man, and cybernetics*, no. 1, pp. 116-132, 1985.
  - [71] N. Kasabov, "Evolving fuzzy neural networks for supervised/unsupervised online knowledge-based learning," *IEEE Transactions on Systems, Man, and Cybernetics, Part B (Cybernetics)*, vol. 31, no. 6, pp. 902-918, 2001.
  - [72] C. Domeniconi and D. Gunopulos, "Incremental support vector machine construction," in *Proceedings 2001 IEEE International Conference on Data Mining*, 2001, pp. 589-592: IEEE.
  - [73] J.-S. Jang, "ANFIS: adaptive-network-based fuzzy inference system," *IEEE transactions on systems, man, and cybernetics*, vol. 23, no. 3, pp. 665-685, 1993.
  - [74] K. Hornik, M. Stinchcombe, and H. White, "Multilayer feedforward networks are universal approximators," *Neural networks*, vol. 2, no. 5, pp. 359-366, 1989.
  - [75] F.T. Abed, H.T.S. ALRikabi, and I.A. Ibrahim, "Efficient Energy of Smart Grid Education Models for Modern Electric Power System Engineering in Iraq," in *IOP Conference Series: Materials Science and Engineering*, 2020, vol. 870, no. 1, p. 012049: IOP Publishing.
  - [76] R.M. Adnan, Z. Liang, A. El-Shafie, M. Zounemat-Kermani, and O. Kisi, "Prediction of Suspended Sediment Load Using Data-Driven Models," *Water*, vol. 11, no. 10, p. 2060, 2019.
  - [77] J. Amudha and D. Radha, "Optimization of Rules in Neuro-Fuzzy Inference Systems," in *Computational Vision and Bio Inspired Computing*: Springer, 2018, pp. 803-818.
  - [78] W. Strauss, "Digital signal processing," *IEEE Signal Processing Magazine*, vol. 17, no. 2, pp. 52-56, 2000.
  - [79] W.K. Jenkins, A.W. Hull, J.C. Strait, B.A. Schnaufer, and X. Li, *Advanced concepts in adaptive signal processing*. Springer Science & Business Media, 2012.
  - [80] J.G. Proakis, J. Catipovic, and M. Stojanovic, "Apparatus for improved underwater acoustic telemetry utilizing phase coherent communications," ed: Google Patents, 1995.
  - [81] J.G. Avalos, J.C. Sanchez, and J. Velazquez, "Applications of adaptive filtering," in *Adaptive Filtering Applications*: InTech, 2011.
  - [82] B. Farhang-Boroujeny, *Adaptive filters: theory and applications*. John Wiley & Sons, 2013.
  - [83] M. Hayes, "The DFT and FFT, the periodogram," *Statistical Digital Signal Processing and Modeling*. John Wiley & Sons, Inc., New York, 1996.
  - [84] S.C. Douglas, "Numerically-robust  $O(N^2)$  RLS algorithms using least-squares prewhitening," in *2000 IEEE International Conference on Acoustics, Speech, and Signal Processing. Proceedings (Cat. No. 00CH37100)*, 2000, vol. 1, pp. 412-415: IEEE.
  - [85] A.H. Sayed and T. Kailath, "A state-space approach to adaptive RLS filtering," *IEEE signal processing magazine*, vol. 11, no. 3, pp. 18-60, 1994.
  - [86] J.A. Apolinário, J.A. Apolinário, and R. Rautmann, *QRD-RLS adaptive filtering*. Springer, 2009.
  - [87] M.H. Hayes, *Statistical digital signal processing and modeling*. John Wiley & Sons, 2009.
-



- [88] F. Wang, X. Yuan, S.C. Liew, and D. Guo, "Wireless MIMO switching: Weighted sum mean square error and sum rate optimization," *IEEE Transactions on Information Theory*, vol. 59, no. 9, pp. 5297-5312, 2013.
- [89] S. Heddam and N. Dechemi, "A new approach based on the dynamic evolving neural-fuzzy inference system (DENFIS) for modelling coagulant dosage (Dos): case study of water treatment plant of Algeria," *Desalination and Water Treatment*, vol. 53, no. 4, pp. 1045-1053, 2015.
- [90] D. Brunet, E.R. Vrscay, and Z. Wang, "On the mathematical properties of the structural similarity index," *IEEE Transactions on Image Processing*, vol. 21, no. 4, pp. 1488-1499, 2011.